

4-2019

Proportion and Evaluation of Ultra-High Performance Concrete Using Local Materials

Flavia Ribeiro Furtado de Mendonca

University of Nebraska-Lincoln, flavia@huskers.unl.edu

Follow this and additional works at: <https://digitalcommons.unl.edu/civilengdiss>

Part of the [Civil Engineering Commons](#), and the [Other Civil and Environmental Engineering Commons](#)

Ribeiro Furtado de Mendonca, Flavia, "Proportion and Evaluation of Ultra-High Performance Concrete Using Local Materials" (2019). *Civil Engineering Theses, Dissertations, and Student Research*. 138.
<https://digitalcommons.unl.edu/civilengdiss/138>

This Article is brought to you for free and open access by the Civil Engineering at DigitalCommons@University of Nebraska - Lincoln. It has been accepted for inclusion in Civil Engineering Theses, Dissertations, and Student Research by an authorized administrator of DigitalCommons@University of Nebraska - Lincoln.

PROPORTION AND EVALUATION OF ULTRA-HIGH PERFORMANCE
CONCRETE USING LOCAL MATERIALS

by

Flávia Ribeiro Furtado de Mendonça

A THESIS

Presented to the Faculty of
The Graduate College at the University of Nebraska
In Partial Fulfillment of Requirements
For the Degree of Master of Science

Major: Civil Engineering

Under supervision of Professor Jiong Hu

Lincoln, Nebraska

April 2019

PROPORTION AND EVALUATION OF ULTRA-HIGH PERFORMANCE CONCRETE USING LOCAL MATERIALS

Flávia Ribeiro Furtado de Mendonça, M.S.

University of Nebraska, 2019

Advisor: Jiong Hu

Ultra-high performance concrete (UHPC) is a new class of concrete that has superior workability, as well as mechanical and durability properties that far exceed those of conventional concrete. To achieve these properties, a very dense internal structure and the very low water-to-binder ratio (w/b) generally are necessary. While particle packing models are typically used to design UHPC, due to the complexity of the composition interaction and characteristics of UHPC, these models might not necessarily provide the best design, which leads to the need of experimental study to justify UHPC performance. The evaluation of the impact of various design parameters on the properties of UHPC is also needed.

A study and evaluation were performed with multiple series of UHPC mixtures prepared with different design parameters and considerations. The impacts of different aggregate, types of fibers, High Range Water Reducing (HRWR), w/b, types of cement, types and quantities of supplemental cementitious materials (SCMs), and different total binder content on UHPC performance were presented.

Furthermore, the extensive amount of fine materials, the absence of coarse aggregate, and the very low w/b often make the process of UHPC production challenging. This study included evaluations of the impacts of mixers on the properties of fresh and hardened UHPC. The comparison of these mixers was used to determine whether mixtures developed in the laboratory were comparable to those used in the field.

ACKNOWLEDGEMENTS

I would like to express my appreciation to my adviser Dr. Jiong Hu for all his input and thoughts in the course of my research. Thank you for encouraging me to believe in myself and continue in the research field. I also would like to thank the support of my committee members Dr. George Morcous and Dr. Yong-Rak Kim, thank you for all comments and suggestions. I wish to acknowledge the Nebraska Department of Transportation (NDOT) for funding the project and providing an opportunity to study UHPC. Thank you, Mrs. Lieska Halsey, Mr. Wally Heyen, Mr. Fouad Jaber, and Mr. Jason Volz. Thanks to Mr. Mostafa Abo El-Khier, Mr. Arman Abdigaliev, Mr. Joey Malloy, and Mr. Miras Mamirov for their valuable assistance in the laboratory.

Table of Contents

| | |
|--|----|
| CHAPTER 1: INTRODUCTION | 1 |
| 1.1 Background | 1 |
| 1.2 Objectives | 2 |
| 1.3 Scope | 3 |
| CHAPTER 2: LITERATURE REVIEW | 4 |
| 2.1 Introduction | 4 |
| 2.2 Background | 4 |
| 2.3 Raw materials | 5 |
| 2.3.1 Cement, Cementitious Materials, and Filler | 5 |
| 2.3.2 Aggregate | 7 |
| 2.3.3 Chemical Admixtures | 9 |
| 2.3.4 Fibers | 10 |
| 2.4 Mixture design | 12 |
| 2.4.1 Particle packing theory | 12 |
| 2.4.2 Other mix design approaches | 14 |
| 2.4.3 Representative UHPC mix designs | 15 |
| 2.5 Mixing | 16 |
| 2.5.1 Mixing energy | 16 |
| 2.5.2 Mixing procedure | 17 |
| 2.6 Properties of UHPC | 18 |
| 2.6.1 Fresh concrete properties | 18 |
| 2.6.2 Hardened concrete | 19 |
| 2.7 Summary | 20 |
| CHAPTER 3: EXPERIMENTAL PROGRAM | 22 |
| 3.1 Introduction | 22 |
| 3.2 Materials | 22 |
| 3.2.1 Cementitious Materials | 22 |
| 3.2.2 Aggregate | 25 |
| 3.2.3 Chemical admixtures | 26 |
| 3.2.4 Fibers | 26 |

| | |
|--|----|
| 3.3 Test Methods..... | 27 |
| 3.3.1 Fresh concrete | 27 |
| 3.3.2 Hardened concrete | 28 |
| 3.4 Mixture development..... | 30 |
| 3.4.1 Experimental approach | 30 |
| 3.4.2 Particle packing theory | 43 |
| 3.5 Mixing..... | 44 |
| 3.5.1 Impact of the mixer..... | 44 |
| 3.5.2 Mixing procedures | 45 |
| 3.6 Summary | 47 |
| CHAPTER 4: RESULTS AND DISCUSSION..... | 49 |
| 4.1 Introduction..... | 49 |
| 4.2 Results and discussion of aggregate, fibers, HRWR, and w/b selection | 49 |
| 4.2.1 Aggregate..... | 49 |
| 4.2.2 Fibers..... | 51 |
| 4.2.3 High Range Water Reducer (HRWR)..... | 52 |
| 4.2.4 Water-to-binder ratio (w/b)..... | 53 |
| 4.3 Results and discussion of the investigation of the binder | 55 |
| 4.3.1 Results..... | 55 |
| 4.3.2 Discussion | 56 |
| 4.4 Particle packing theory | 66 |
| 4.5 Results and discussion of the impact of different mixers and mixing procedures.. | 67 |
| 4.6 Summary | 70 |
| CHAPTER 5: SUMMARY, CONCLUSIONS, AND FUTURE WORK | 72 |
| 5.1 Conclusions..... | 72 |
| 5.2 Future work..... | 74 |
| 5.2.1 Particle packing and further mixture development..... | 74 |
| 5.2.2 Rheology of UHPC | 75 |
| CHAPTER 6: REFERENCES | 84 |

List of Tables

| | |
|--|----|
| Table 2.1. Maximum aggregate particle size | 8 |
| Table 2.2 Types and dimensions of fibers reportedly used in UHPC..... | 10 |
| Table 2.3. Representative UHPC mix design from agencies..... | 16 |
| Table 3.1. Chemical composition of cement and the types of SCMs | 24 |
| Table 3.2. Physical and mechanical properties of fibers | 27 |
| Table 3.3. Mix design of mixes prepared with different fibers | 35 |
| Table 3.4. Mix design of mixes prepared with different HRWRs | 36 |
| Table 3.5. Mix design of mixes prepared with different w/b values | 37 |
| Table 3.6. Mix design prepared with different types of cement | 39 |
| Table 3.7. Mix design of the mixes prepared with different contents of silica fume | 40 |
| Table 3.8. Mix design of mixes prepared with fly ash..... | 41 |
| Table 3.9. Mix design of the mixes prepared with slag | 41 |
| Table 3.10. Mix design of the mixes prepared with quartz powder | 42 |
| Table 3.11. Mix design of mixes prepared with different total binder contents | 43 |
| Table 3.12. Mix design of mixes using different mixers | 45 |
| Table 4.1. Results of mixes in the investigation of the binder..... | 56 |
| Table 4.2. Impact of different mixers | 68 |
| Table 5.1. Concrete unit weight using different consolidation method..... | 83 |

List of Figures

| | |
|---|----|
| Figure 2.1 Frequency of maximum aggregate size used in UHPC..... | 9 |
| Figure 2.2. Typical fibers used in UHPC..... | 11 |
| Figure 2.3. Difference between normal concrete and the structure of UHPC | 12 |
| Figure 3.1. Particle size distribution of cement and various types of SCMs | 24 |
| Figure 3.2. Particle size distribution of aggregates..... | 26 |
| Figure 3.3. Fibers used in the study. | 27 |
| Figure 3.4. Flow table | 28 |
| Figure 3.5. Machine used for mechanical property testing. | 29 |
| Figure 3.6. Flexural strength test setup and typical results..... | 30 |
| Figure 3.7. Flow chart of mixture development. | 31 |
| Figure 3.8. Cement and SCMs types and quantities used in stage 3 study..... | 38 |
| Figure 3.9. Flow charts of the batching and mixing procedure for different sizes of batches..... | 46 |
| Figure 3.10. Comparison of changes in the mixers and the consistency during mixing: | 47 |
| Figure 4.1. Uncompacted and compacted voids of aggregates in the No. 10 sand matrix | 50 |
| Figure 4.2. Load-displacement relationship of the flexural behavior of UHPC with different types of fibers | 51 |
| Figure 4.3. Examples of UHPC mixtures with different consistencies | 52 |
| Figure 4.4. Impact of w/b on UHPC performance. | 54 |
| Figure 4.5. Impacts of the types of cement on the performance of the UHPC..... | 57 |
| Figure 4.6. Impact of the silica fume content on the performance of the UHPC | 58 |
| Figure 4.7. Comparison of effects of undensified and densified silica fume on the performance of the UHPC | 60 |
| Figure 4.8. Impact of fly ash on the performance of UHPC..... | 61 |
| Figure 4.9. Impact of slag on the performance of the UHPC | 62 |
| Figure 4.10. Impact of quartz powder in the UHPC performance..... | 63 |
| Figure 4.11. Impact of the binder content on UHPC performance..... | 65 |
| Figure 4.12. Particle packing curve of mixes mixed with different total binder content . | 66 |
| Figure 4.13. Impact of mixers on the performance of the UHPC..... | 69 |
| Figure 5.1. Comparison of the results of static and dynamic flow. | 77 |
| Figure 5.2. Distribution and Orientations of the fibers..... | 79 |
| Figure 5.3. Orientations of the fibers in broken beams..... | 81 |

CHAPTER 1: INTRODUCTION

1.1 Background

Ultra-high performance concrete (UHPC) is a new class of concrete that has superior flowability, as well as mechanical and durability properties. The low water-to-binder ratio (w/b), high binder content, the use of steel fibers, and the absence of coarse aggregate make UHPC significantly different from conventional concrete in both the fresh and hardened states. Since the use of UHPC will result in significant improvements in the structural capacity and durability of structural components, various issues, such as cracking and leakage in bridge connections, can be mitigated to a significant extent.

The superior strength and durability properties are general due to the optimized particle packing of the materials. UHPC's components are selected rigorously considering the sizes and distributions of particles to maximize their packing density (El-Tawil et al., 2016). A high packing density is obtained when the particles are arranged so that the voids of the matrix are minimized. UHPC's design generally is based on the optimum particle packing so that the materials in the matrix are combined in optimum proportions, thereby minimizing voids and ensuring high strength, i.e., a minimum of 17,000 psi (120 MPa), low permeability, and self-consolidating nature (Yu et al., 2015; Lowke et al., 2012).

Different approaches are being used to design UHPC, and particle packing models are commonly used. However, because the particle sizes of fine powders, such as cement and supplemental cementitious materials (SCMs) are so small, they are subjected to strong interparticle forces, which generally does not take into account in the models.

Thus, while particle packing models can serve as a general guideline, experimental work is still necessary to determine the actual packing for optimum UHPC design. The study, therefore, evaluated the impact of different parameters on the UHPC performance experimentally.

The current use of UHPC in the U.S. is limited to proprietary, pre-packed products provided by international suppliers because of the highly-sophisticated design of the mixture, the mixing procedure, and in some cases, the limited availability of raw materials. The high costs of the materials associated with these products, which can be as much as \$2,000 per cubic yard plus the costs associated with batching, placing, and curing, have been a major impediment for the extended use of UHPC. Therefore, through the examination of the impact of different parameters on the UHPC performance, a non-proprietary UHPC mix based on local materials is proposed. Since the mixing process is intense and important for the production of UHPC, a comparison study of mixtures produced with different mixers and the control of consistency during the UHPC mixing process also are presented.

1.2 Objectives

The objectives of this study were to evaluate the impact of different materials and design parameters on UHPC performance and to proportion a non-proprietary UHPC mix using local materials. A methodology to proportion the materials is presented, and key parameters, e.g., the w/b, the type of binder and its content, gradation of the aggregate, types of fibers, HRWR, and the type of mixer were evaluated.

1.3 Scope

This research was divided into four main parts. The first part, presented in Chapter 2, includes an extensive literature review. Limitations regarding the approaches that were used for designing the mix are noted. The preliminary materials and the mixing procedure selected to develop the UHPC used in this study were determined based on information acquired from the literature review and availability.

The second part is the experimental program presented in Chapter 3, which includes the selection of the candidate materials, the adjustment of the proportions of the materials, and the test methods used in the mixes. Chapter 4 presents the performance of UHPC with different types of materials and contents, and the results are discussed. Chapter 5 includes a summary of the research, the conclusions, and recommendations for future work.

CHAPTER 2: LITERATURE REVIEW

2.1 Introduction

During the last decade, due to the superior properties of UHPC, extensive research has been conducted to develop UHPC with different materials and different design approaches. This chapter provides a summary of the materials that typically are used in UHPC, approaches and examples in designing the UHPC mix, and the properties of the UHPC.

2.2 Background

The concept of having a high-strength, high-performance, cementitious material was initiated in the 1970s based on the better understanding of hydration reactions, shrinkage, creep, and porosity, as well as the development of water reducers and advanced curing processes. The terminology related to high strength concrete was developed in the 1980s when concrete materials with compressive strengths up to 8,702 psi (60 MPa) were developed using supplemental cementitious materials (SCMs) and the water-to-cement ratio (w/c) was reduced. In addition, high-strength concrete, with its improved durability properties, was designated as high-performance concrete. UHPC initially was introduced in the early 1990s with the application of particle packing theory, the use of fine particles, low porosity, and low w/c. Advances in the development of chemical additives and the introduction of various different fibers in the concrete also contributed to the development and use of UHPC (Naaman and Wille, 2012).

Different institutions have different requirements that characterize UHPC. ASTM C1856 (ASTM, 2017) specifies a minimum compressive strength of 17,000 psi (120

MPa), maximum aggregate nominal size of aggregate of ¼ in (5 mm), and flow between 8 and 10 in (200 and 250 mm) measured using the flow table test. However, Federal Highway Administration (FHWA) (Haber et al., 2018), and American Concrete Institute ACI 239 (ACI 239R-18, 2018) defines UHPC as a cementitious composite material composed of an optimized gradation of granular constituents, w/c less than 0.25, and a high percentage of discontinuous internal fibers reinforcement. The mechanical properties of UHPC include compressive strength greater than 21,700 psi (150 MPa) and sustained post-cracking tensile strength greater than 720 psi (5 MPa).

According to ACI 239 (ACI 239R-18, 2018), the high performance of UHPC is due to its discontinuous pore structure and the reduced void space in the matrix. It is implied that the level of stress transferred between particles is reduced when the contact points between particles are increased. Thus, the proper selection of materials is very important. The reduction of the level of stress improves the mechanical properties because it alleviates the formation of microcracks. Also, UHPC is expected to have a discontinuous pore structure, which reduces the ingress of liquids and significantly enhances its durability compared to conventional concrete.

2.3 Raw materials

2.3.1 Cement, Cementitious Materials, and Filler

For non-proprietary UHPC, the general ingredients are cement, pozzolanic reactive materials, i.e., SCMs, filler, fine aggregate, superplasticizer, and fibers. Cement is the principal binder in UHPC, and the SCMs improve the particle packing, resulting in a denser structure and enhancing the strength due to the pozzolanic reactions. Sometimes, fillers also are used to improve the packing.

Cement accounts for approximately 20% of the total volume of the concrete. The main chemical compounds of Portland cement are C_3S , C_2S , C_3A , and C_4AF . When C_3S and C_2S are hydrated, they are the main contributors to the strength of concrete. According to Sakai et al. (2008), the hydration process of C_3A occurs rapidly due to its high surface area, and this results in an increase in the demand for water demand, which consequently affects the apparent viscosity of the fresh concrete. Thus, a low amount of C_3A can reduce the required amount of water, the formation of ettringite, and the heat of hydration (Shi et al., 2015). Therefore, cement with a C_3A content less than 8% is desirable in UHPC mixes. Willi et al. (2011 (a)) concluded that cement with a low amount of C_3A , high amounts of C_3S and C_2S , and moderate fineness provide good performance for UHPC. Most researchers use Type I/II Portland cement due to its low content of C_3A . There also have been reports of the use of other types of cement, such as Type III cement, because it has smaller particles than Types I/II cement. Note that, since the cement in UHPC usually is not fully hydrated, the remaining unhydrated particles can be considered as filler when cement with finer particles is used (Meng et al., 2017(b)). In addition, Class H oil well cement has been used due to the better overall packing and its coarser particle size, which enhance late age strength (Harber et al., 2018; Muzenski, 2015; Scott et al., 2015).

Silica fume, a byproduct from the production of ferrum-silicium alloys, is a common pozzolanic material used for the fabrication of UHPC. This product can improve the packing density of the matrix and prevent the formation of pores in the UHPC. During the pozzolanic reaction, silica fume reacts with $Ca(OH)_2$ from the hydration of cement, forming C-S-H, which is the main hydration product responsible for the strength

of concrete. According to Scrivener (2004), silica fume also can improve the interfacial transition zone of the concrete by reducing its porosity in early ages. Various researchers have suggested different contents of silica fume since, despite its advantages, it can decrease the workability of the UHPC due to its high surface area and the resulting high demand for water.

Fly ash is one of the most extensively used SCMs in concrete. It is a byproduct of coal-burning electric power plants with most of the particles solid spheres or hollow cenospheres (Kosmatka et al., 2003). Fly ash can improve the workability of UHPC due to its lubricating and ball bearing effects (Meng, 2017). The pozzolanic reactions of fly ash can improve the UHPC's mechanical properties.

Ground, granulated blast-furnace slag, also called slag, is another SCM that commonly is used in UHPC (Meng, 2017; Yu et al., 2015; Wille et al., 2011 (b)). Generally, the slag particles have rough and angular shapes, and, in the presence of water and cement, the slag hydrates and sets, similar to Portland cement (Kosmatka et al., 2003).

In addition to the materials mentioned, some other materials, such as glass powder (Naaman and Wille, 2012) and quartz powder (Haber et al., 2018) also have been used in UHPC because it is believed that they can provide better particle packing of the UHPC.

2.3.2 Aggregate

Coarse aggregates are not normally used in UHPC. According to De Larrard and Sedran (1994), in order to improve the strength of UHPC, it is desirable to use only fine sand as aggregate, due to the influence of maximum paste thickness (MTP), which represents the mean distance between two aggregates when they are surrounded by

| Maximum size of the aggregate | Wille et al., 2011 (b) | Naaman et al., 2012 | Ambily et al., 2014 | Yu et al., 2014 (a) | Yu et al., 2014 (b) | Yu et al., 2015 | Alkasy et al., 2015 | Meng et al., 2016 | Wu et al., 2016 | Meng et al., 2017 |
|-------------------------------|------------------------|---------------------|---------------------|---------------------|---------------------|-----------------|---------------------|-------------------|-----------------|-------------------|
| 0.106mm | | | | | | | YES | | | |
| 0.150mm | | YES | YES | | | | | | | |
| 0.500mm | | | | | | | YES | | | |
| 0.800mm | | YES | | | | | | | | |
| 1.000mm | | | | YES | YES | YES | | | | |
| 2.000mm | YES | | | | | | | YES | | YES |
| 2.360mm | | | YES | YES | YES | YES | | | YES | |
| 4.750mm | | | | | | | | YES | | YES |

| Maximum size of the aggregate | Wille et al., 2011 (b) | Naaman et al., 2012 | Ambily et al., 2014 | Yu et al., 2014 (a) | Yu et al., 2014 (b) | Yu et al., 2015 | Alkasy et al., 2015 | Meng et al., 2016 | Wu et al., 2016 | Meng et al., 2017 |
|-------------------------------|------------------------|---------------------|---------------------|---------------------|---------------------|-----------------|---------------------|-------------------|-----------------|-------------------|
| 0.106mm | | | | | | | YES | | | |
| 0.150mm | | YES | YES | | | | | | | |
| 0.500mm | | | | | | | YES | | | |
| 0.800mm | | YES | | | | | | | | |
| 1.000mm | | | | YES | YES | YES | | | | |
| 2.000mm | YES | | | | | | | YES | | YES |
| 2.360mm | | | YES | YES | YES | YES | | | YES | |
| 4.750mm | | | | | | | | YES | | YES |

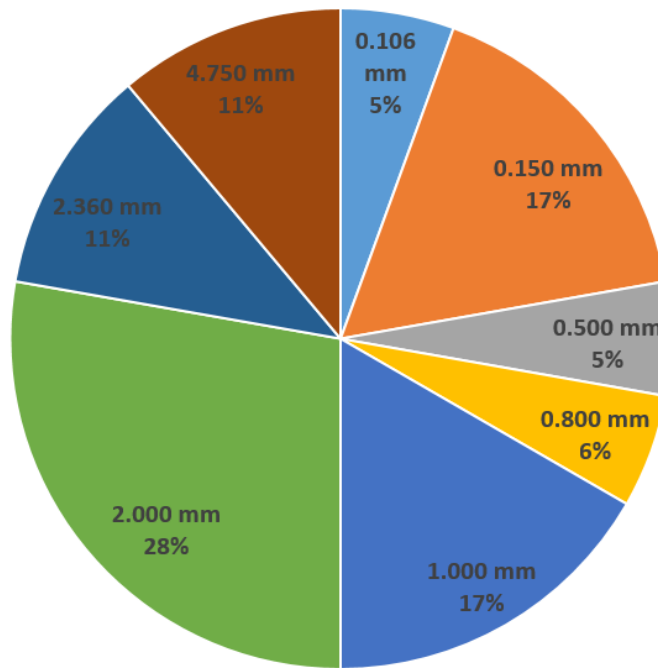


Figure 2.1 Frequency of maximum aggregate size used in UHPC

2.3.3 Chemical Admixtures

The chemical admixture that is used most commonly in UHPC is the high-range, water-reducing (HRWR) admixture, which also is called ‘superplasticizer.’ The HRWR admixture reduces the amount of water required in the mix. Since the w/b of UHPC can be as low as 0.16, the admixture is very important to ensure the workability to the fresh concrete. According to Schrofl et al. (2008), polycarboxylate ether-based HRWR is a more effective superplasticizer for UHPC, and other types of HRWR, such as phosphonate-based HRWR, also have been reported. HRWR can have different chains lengths, but the differences sometimes can delay the setting time of the concrete (Wille, 2011). Therefore, accelerators sometimes are used in UHPC to ensure appropriate early age strength for construction (Graybeal, 2014).

2.3.4 Fibers

According to Graybeal (2014), the addition of fibers to the UHPC improves the hardened concrete characteristics and it is very important when it is used in structural elements. It can increase the tensile capacity and ductility and reduce the propagation of cracks. The materials, dimensions, and shapes of the fibers vary depending on the availability of materials. Table 2.2 shows the reported types of fibers used in UHPC and their dimensions.

Table 2.2 Types and dimensions of fibers reportedly used in UHPC

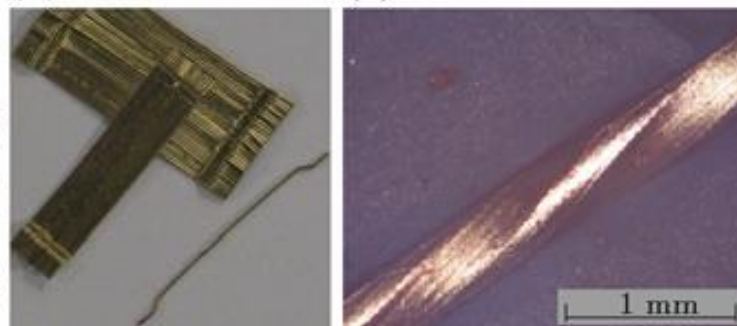
| Type | Diameter (in) | Length (in) |
|------------------|---------------|-------------|
| Straight steel | 0.008 | 0.748 |
| | 0.008 | 0.512 |
| | 0.006 | 0.236 |
| End-hooked steel | 0.015 | 1.181 |
| Twisted steel | 0.012 | 0.709 |
| | 0.005 | n/a |
| PVA | 0.002 | 0.472 |
| | 0.002 | 0.315 |
| | 0.012 | n/a |

1 in = 25.4 mm

The type of fibers that is used most often is steel fibers with diameters that range from 0.006 in (0.152 mm) to 0.015 in (0.381 mm) and lengths that range from 0.236 in (6 mm) to 1.181 in (30 mm). They can be end-hooked, straight, or twisted. Among the steel fibers, the straight steel fibers with diameters of 0.008 in (0.200 mm) and lengths of 0.512 in (13 mm) long are used most often for UHPC.

Table 2.2 shows that some researchers have used PVA and polyethylene fibers in UHPC (Sbia et al., 2014; Nebraska Concrete Paving Association, n/a; Japan Society, 2008; Khayat and Meng, 2017). The combination of different types of fibers or dimensions has been reported as being used in UHPC to achieve the desired performance (Shi et al., 2015; Sbia et al., 2014).

Fibers are important to ensure desirable mechanical properties, particularly toughness and post-cracking tensile strength. However, since the use of fibers impacts the packing of the particles and increases the surface area of the solid particles in the mix, which lead to changes in the properties of fresh UHPC, the proportion of fibers in the concrete must be controlled carefully. Meng et al. (2017) reported that 2% of fibers by volume is considered to be the optimum fiber content for UHPC to provide the desired hardening properties. Figure 2.2 shows some different types of steel fibers that are used in UHPC.



(a) Hook-ended steel fiber (b) Twisted steel fiber fiber

(Wille and Naaman, 2012)



(c) Straight steel fiber (d) PVA fiber

(El-Tawil et al., 2017)

Figure 2.2. Typical fibers used in UHPC.

2.4 Mixture design

2.4.1 Particle packing theory

It is well known that the particle size distribution affects both the fresh and hardened properties of concrete (Hunger and Brouwers, 2006). In UHPC, the high-density packing of particles is desired in order to achieve high strength and low permeability. The UHPC design is achieved when the materials of the matrix are combined in optimal proportions, and the voids between the particles are minimized (Yu et al., 2015; Lowke et al., 2012). In order for UHPC to have sufficient strength, the mixes generally are designed based on particle-packing theory, which is considered as the design philosophy for UHPC (El-Tawil, 2018). The particle-packing theory is based on decreasing the porosity of the concrete by filling the voids between the larger particles in the matrix with smaller particles, thereby reducing the number of voids. Figure 2.3 shows a schematic depiction of the difference between the matrix structure of normal concrete and UHPC. The UHPC structure is packed densely with minimum voids between the particles, while the structure of normal concrete is loosely packed.

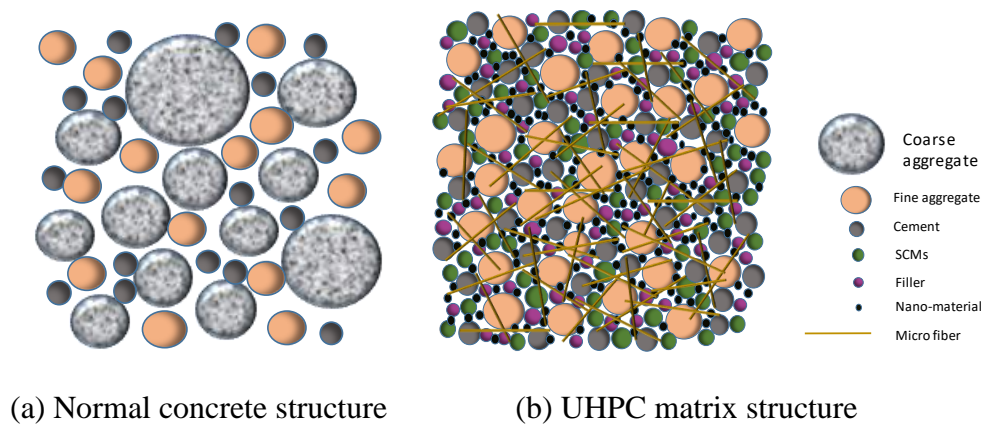


Figure 2.3. Difference between normal concrete and the structure of UHPC

According to Hunger and Brouwers (2006), many particle packing models are available. The Andreasen and Andersen (A&A) theory, as shown in Equation 2.1, is the most commonly used model to design UHPC.

$$P(D) = \frac{D^q}{D_{max}^q} \quad \text{Equation 2.1}$$

where D is the particle size (μm); $P(D)$ is the volume fraction of the total solids smaller than size D ; D_{max} is the maximum particle size (μm); and q is the distribution modulus.

Since the A&A model does not account for the minimum particle size, a modified Andreasen and Andersen model was developed (Yu et al., 2014 (b)), and it is considered to be more appropriate for mixtures with fine materials, such as UHPC. The modified model considers both the maximum and minimum sizes of the particles of the material. Based on the modified A&A particle packing theory, an optimum curve can be generated based on Equation 2.2.

$$P(D) = \frac{D^q - D_{min}^q}{D_{max}^q - D_{min}^q} \quad \text{Equation 2.2}$$

where D is the particle size (μm); $P(D)$ is the volume fraction of the total solids smaller than size D ; D_{max} is the maximum particle size (μm); D_{min} is the minimum particle size (μm); and q is the distribution modulus. Theoretically, q should be in the range of 0 to 0.28 for fine granular blends (Hunger and Brouwers, 2006). According to Huger (2010), small q values are more suitable for finer packing, as in the case of UHPC. A q value of 0.23 was selected in this study based on the previous study by Yu et al. (2015).

Although the particle packing theory model often is used to design UHPC, fine powders, such as cement and SCMs, are subjected to strong interparticle forces due to their high fineness, which generally is not accounted for in the model. Also, when liquid

is introduced in the mix, the interaction force between fine particles (<0.004 in $(100\ \mu\text{m})$) is affected, which also generally is not accounted for (Meng et al., 2017). Also, other factors that could affect the degree of particle packings, such as particle shape and surface condition are not considered in most packing models. Thus, while particle packing theory can serve as a general guideline, experimental work is still necessary with the specific materials used to determine the actual packing for optimum UHPC design.

2.4.2 Other mix design approaches

In addition to particle packing theory models, different methods have been used in designing UHPC. In order to improve particle packing, some researchers (Wille et al., 2011; Graybeal, 2013; Meng et al., 2017) used combinations of different aggregates. It was reported that bulk density or a particle packing model could be used to define the best proportion of aggregates to be used.

Some researchers (Wille et al., 2011; Graybeal, 2013) used multiple stages to obtain the most promising cement paste, and then they incorporated the aggregate and the fibers. First, cement pastes with the best flowability and compressive strength were identified by adjusting the cement and SCMs, w/b, and HRWR. Then, appropriate amounts and types of aggregates and fibers were introduced to obtain mixtures with promising workability and mechanical characteristics.

Their approach, however, did not evaluate the packing density of the entire UHPC matrix, i.e., the paste and aggregate together. It assumed that the best performing paste would provide the best performing UHPC. Although the paste significantly affects the workability and compressive strength of UHPC, the particle packing could be disturbed when the aggregate is introduced. The combined packing of aggregates and powder

materials is a key parameter in the performance of UHPC. Therefore, even though it is a reasonable method, the packing density of the entire matrix, including the paste and the aggregate, should not be neglected. The energy required to mix the cementitious paste will be different from the energy required to mix UHPC, and the different mixing energies can result in the final products having different performances.

Berry et al. (2017) defined the proportion of UHPC materials using a response surface methodology (RSM). They developed trial batches to collect sufficient data to create a model that consisted of a set of complex regression equations that can predict the behavior of each of the components of the UHPC mix. Although it was stated that the method could accurately provide responses of the behaviors and interactions of the constituents, trial batches are required to build the model, and this can become impractical.

2.4.3 Representative UHPC mix designs

As mentioned previously, the UHPC design usually consists of dry constituents, i.e., cement, SCMs, filler, fine aggregate, fiber, and liquid, i.e., water, and HRWR. Table 2.3 shows some typical examples of mix designs from the research projects of federal and state agencies. In UHPC mixes, the binder content has an average of 1800 pcy (1068 Kg/m³), and the average w/b is 0.164.

Table 2.3. Representative UHPC mix design from agencies

| Constituent | FHWA (Haber et al., 2018) | Michigan (El-Tawil et al., 2018) | Montana (Berry et al., 2017) | Missouri (Meng et al., 2017) |
|---------------|---------------------------------|--|------------------------------------|------------------------------------|
| Cement | 1328 | 653 | 1300 | 924 |
| Slag | NA | 653 | NA | 902 |
| Fly Ash | NA | NA | 371 | NA |
| Silica Fume | 518 | 327 | 279 | 71 |
| Ground Quartz | 367 | NA | NA | NA |
| Fine Sand | NA | 394 ¹ | NA | 512 ⁴ |
| Coarse Sand | 1288 | 1577 ² | 1556 ³ | 1170 ⁵ |
| HRWR | 23 | 39 | 272 | 282 |
| Water | 278 | 264 | 60 | 27 |
| Steel Fibers | 416 | 265 | 263 | 263 |

Note: All values are presented in pcy (1 pcy = 0.59 Kg/m³)

1-U.S. Silica F75, max. particle size = No. 40 (0.425 mm)

2- U.S. Silica F12, max. particle size = No. 30 (0.6 mm)

3- Masonry sand, washed and dried max. particle size = No. 8 (2.36 mm)

4- Masonry sand, max. particle size = No. 10 (2 mm)

5- Missouri river sand, max. particle size = No. 4 (4.75 mm)

2.5 Mixing

2.5.1 Mixing energy

As stated previously, the loading procedure and mixing time of UHPC are very important to ensure uniformity and consistency. The energy required to mix UHPC is higher than it is to mix normal concrete, so a longer mixing time generally is necessary to achieve the desired consistency and performance. Due to the very fine particles and low w/b in UHPC, clumps are formed easily during the mixing (El-Tawil et al., 2017). High-shear pan mixers generally are preferable to increase the efficiency of the mixing process (Graybeal, 2014). Such mixers usually have paddles that help scrape materials off of their walls.

Different paddles, dimensions of mixers, and mixing speeds provide different energy inputs. El-Tawil et al. (2017) measured the flow and turnover time (time when a

consistency of UHPC mix was observed, i.e., when the materials start to change from powder form to liquid form) for UHPC prepared with different processes. It was observed that the mixing speed influenced the performance of the fresh concrete. As the mixing speed increased, the UHPC workability increased slightly, and the turnover time decreased drastically. Therefore, different mixing procedures may be necessary for field mixing when the rotation speed of the mixer is lower.

2.5.2 Mixing procedure

Because of the high content of fine particles and the intensive energy required for mixing, the sequence of loading materials and the mixing procedure for UHPC are very important to achieve the desired fresh and hardened properties. Different researchers have different approaches for the mixing procedure, but the process generally can be separated into three steps, i.e., (1) mix the dry components, (2) add water and HRWR, and (3) add fibers. Some researchers (Yu et al., 2014, 2015; Bonneau et al., 1997; Ambily et al., 2014; Meng et al., 2016, 2017; Wu et al., 2016; Yang et al., 2009; Shi, 2015) have suggested that all of the powder and aggregate first should be mixed for 30 seconds to 10 minutes. Then, it was suggested that water and HRWR should be added to the mixture. In some cases, the water is divided into two portions and loaded separately into the mixer to enhance its dispersion (Yu et al., 2014, 2015; Meng et al., 2016, 2017). After the liquid is added, the total mixing time varies from 5 to 12 minutes. Then, the fibers are added. Other researchers (Wille et al., 2011; Alkaysi, 2015; Naaman et al., 2012; Graybeal, 2013) suggested dry mix silica fume and aggregate first for 5 minutes to ensure the breakdown of the particles of the silica fume. Then, cement and SCMs are added and mixed for 5 more minutes. After that, water and HRWR are added slowly into the mixer

and mixed until the concrete reaches the expected consistency. Finally, fibers are added and mixed for 5 minutes to ensure their dispersion. Based on the results of the trial experiments, this procedure was adjusted and used in this study.

De Larrard and Sedran (1994) suggested mixing the powder and the liquid first until a homogenous slurry is observed and then add the sand. According to Ferdosian and Camoes (2016), this procedure can help produce a lower viscosity mixture because the water in contact with cement in the initial stage of mixing releases Ca^{2+} ions that subsequently are absorbed onto the HRWR chain. El-Tawil et al. (2017) affirmed that this procedure could reduce the demand for the extensive use of power for mixing during the mixture turnover stage, reducing the probability of a malfunction of the mixer. However, the authors suggested a different procedure that involved dividing the sand into two portions, adding the first portion with the powder materials and mixing for 5 minutes, followed by the addition of the liquid, and after the concrete turnover, add the second portion of sand and finally the fibers. It was shown that the sand helps to mix and disperse the materials, thereby shortening the turnover time of the mixture.

2.6 Properties of UHPC

2.6.1 Fresh concrete properties

UHPC has highly flowable, thus the control of the fresh properties requires consistent measurements of the workability. The properties of fresh UHPC normally are determined using the flow table test (Naaman and Wille, 2012; Meng et al., 2017; Choi et al., 2016), which consists of filling a small, cone-shaped mold atop a standard flow table, raising the mold from the mixture, and measuring the spread. However, different procedures after raising the mold from the mixture are suggested by different

specifications. For instance, according to ASTM C1437 (ASTM, 2015), the test consists of dropping the table 25 times in 15 seconds and calculating the average of the diameters measured from the four lines scribed in the top of the table. The Federal Highway Administration (Haber et al., 2018) suggested a different approach that involved letting the concrete flow by itself until no movement is detected and then calculating the average of the diameters measured from the four lines scribed in the flow tabletop; this measurement is reported as the “static” flow. Immediately afterward, 20 drops are applied to the table, and, then, the average of the diameters of the four lines scribed in the table top is calculated and reported as the “dynamic” flow. The new ASTM C1856 (ASTM, 2017) standard for UHPC states that the material must be allowed to spread by itself for 2 minutes, after which the average between the maximum and minimum diameters is to be calculated. Different state and federal agencies have been using a 7 to 10 in (179 to 250 mm) flow as the criterion for UHPC flow, while ASTM 1856 requires 8 to 10 in (200 to 250 mm).

In addition to the flow table tests, other tools, such as rheometers (Dils et al., 2013) and mini V-funnels (Meng, 2017; Dils et al., 2013), have been used to evaluate the workability and rheological behavior of UHPC. However, their use is limited significantly due to the lack of availability of the instruments.

2.6.2 Hardened concrete

The uniaxial compressive strength of UHPC can reach a high value of 30,000 psi (206 MPa) depending on the materials, the technologies used in the mixing procedure and the curing process, and age. Thus, with the superior properties of UHPC, similar

structural requirements of normal reinforced concrete can be achieved with less reinforcement and less concrete.

While different agencies and organizations have specified different minimum compressive strengths for UHPC, the compressive strength of non-proprietary UHPC after 28 days varies from 11,300 psi to approximately 30,000 psi (77.9 MPa to 206 MPa). The flexural strength of UHPC is enhanced due to the addition of the fibers that commonly are used in the development of UHPC, and the reported 28-day flexural strength varies from 1,800 psi to 5,000 psi (12.4 MPa to 34.4 MPa).

2.7 Summary

This chapter presents the results of the literature review that was conducted for this research. Based on the literature review, preliminary materials were selected for further analysis. The loading sequence and mixing procedure that were used in this research for the production of UHPC also were based on the findings from the literature review.

Although different approaches have been reported for the design of UHPC, all of them have issues. In addition, the particle packing model that was used to design UHPC was the modified A&A model. However, this model only considers dry particles, and it does not account for the interaction force between fine particles in dry and wet conditions. Also, the shapes and textures of the particles were not taken into account. Other approaches optimize the paste of the UHPC independently of the aggregate, but they disregarded the overall matrix packing density of UHPC. Instead, the packing density of the paste was optimized separately from the optimization of the aggregate matrix, and the two materials were combined later. Besides the concern of the particle

packing density, the energy used to mix the paste can be different from the energy required to mix the mortar, which, consequently, results in a different performance of the final product. It is important to implement a better method that simultaneously accounts for the cementitious materials paste, the aggregate, and the fibers.

The fresh and hardened properties of the UHPC and the test methods are presented in this chapter. The most-frequently test used to measure the UHPC fresh property is the flow table test, which is an empirical test to evaluate the rheological parameters of the concrete. Thus, a more scientific test, such as the use of rheometers, is needed to help answer questions. Also, different methods of measuring flow are suggested, and this inconsistency must be addressed.

CHAPTER 3: EXPERIMENTAL PROGRAM

3.1 Introduction

The object of this chapter is to present the materials and mix designs of UHPC mixtures, the tests that were performed, and the experimental program that was used to develop the mixes. Also, the different mixing procedures used in the study are presented.

The different types of cement, SCMs, aggregates, fibers, and chemical admixtures used in the study are presented. Most of the materials presented were selected based on a review of the literature review and their availability.

This chapter also includes the test methods that were used to evaluate the fresh and hardened properties of UHPC, such as flowability, compressive strength, and flexural strength. The tests of flowability and compressive strength are essential to determine whether the UHPC mixes that were developed are acceptable according to the requirements of ASTM 1856 (ASTM, 2017).

The process of defining the proportions of the UHPC mixtures is presented in this chapter. The methodology of proportioning the materials was based on experiments, which means that the impacts of various parameters were evaluated, such as w/b, type and content of the binder, HRWR, and fibers in the UHPC mixes. The impacts of different mixer on the performance of the UHPC also are presented in this chapter.

3.2 Materials

3.2.1 Cementitious Materials

Because of the much higher binder content compared to conventional concrete, the cementitious materials used for UHPC should be selected rigorously due to their

contribution to the fresh and hardened properties of the final product. The workability and the strength of UHPC depend significantly on the type of binder and its content. While fresh cement paste controls the workability of UHPC, the hydration of the cement and the pozzolanic reactions of SCMs determine the properties of the hardened product.

3.2.1.1 Cement

In this research, four types of cement were used in the development of UHPC, i.e., Type I/II Portland cement, Type III Portland cement (both of which meet ASTM C150 (ASTM, 2018)), Type IP Portland cement that meets ASTM C595 (ASTM, 2018), and Class H Oil Well cement that meets American Petroleum Institute API – Spec 10A (API, 2010).

3.2.1.2 Supplemental Cementitious Materials and Filler

Various products were used for SCMs, i.e., 1) class C fly ash that meets ASTM C618 (ASTM, 2017), 2) densified silica fume and undensified silica fume that meet ASTM C1240 (ASTM, 2015), and 3) ground, granulated blast-furnace slag that meets ASTM C989 (ASTM, 2018). A quartz powder also was used in the study as a filler material.

The chemical composition and the particle size distribution curves for the different types of cement and SCMs used are shown in Table 3.1 and Figure 3.1, respectively.

Table 3.1 Chemical composition of cement and the types of SCMs

| Substance | Content (%) | | | | | | | |
|--|------------------|----------------|-----------------|-------------------------|---------|-------------|-------|---------------|
| | Type I/II Cement | Type IP Cement | Type III Cement | Class H Oil Well Cement | Fly ash | Silica Fume | Slag | Quartz Powder |
| Silicon Dioxide (SiO ₂) | 20.4 | - | 19.50 | 21.90 | 42.46 | 92.50 | - | 99.40 |
| Silicon trioxide (SiO ₃) | - | - | - | - | - | 0.52 | 0.04 | - |
| Aluminum Oxide (Al ₂ O ₃) | 4.10 | - | 4.60 | 4.20 | 21.00 | - | - | 0.26 |
| Iron Oxide (Fe ₂ O ₃) | 3.10 | - | 3.20 | 5.00 | 4.78 | - | - | 0.031 |
| Sulfur Trioxide (SO ₃) | 2.70 | 3.10 | 3.40 | 2.40 | 1.12 | - | - | - |
| Calcium Oxide (CaO) | 63.80 | - | 62.3 | 64.20 | 20.34 | - | - | 0.01 |
| Magnesium Oxide (MgO) | 2.30 | 2.45 | 4.00 | 1.10 | 3.69 | - | - | 0.02 |
| Sodium Oxide (Na ₂ O) | 0.12 | - | - | 0.09 | 1.43 | - | - | <0.01 |
| Potassium Oxide (K ₂ O) | 0.71 | - | - | 0.66 | 0.62 | - | - | 0.03 |
| Carbon dioxide (CO ₂) | 1.70 | - | 1.90 | - | - | - | - | - |
| Limestone | 4.30 | - | 4.50 | - | - | - | - | - |
| CaCO ₃ in Limestone | 88.00 | - | 94.00 | - | - | - | - | - |
| Titanium dioxide | - | - | - | - | - | - | - | 0.01 |
| Chlorine (CL ⁻) | - | - | - | - | - | 0.14 | - | - |
| C ₃ S | 60.00 | - | 51.00 | 52.00 | - | - | 0.84 | - |
| C ₂ S | 13.00 | - | 17.00 | 24.00 | - | - | 55.30 | - |
| C ₃ A | 6.00 | - | 7.00 | 3.00 | - | - | 7.90 | - |
| C ₄ AF | 9.00 | - | 10.00 | 15.00 | - | - | 8.80 | - |
| Loss-on-Ignition | - | 1.00 | 2.50 | 1.10 | 0.75 | 3.39 | - | 0.30 |

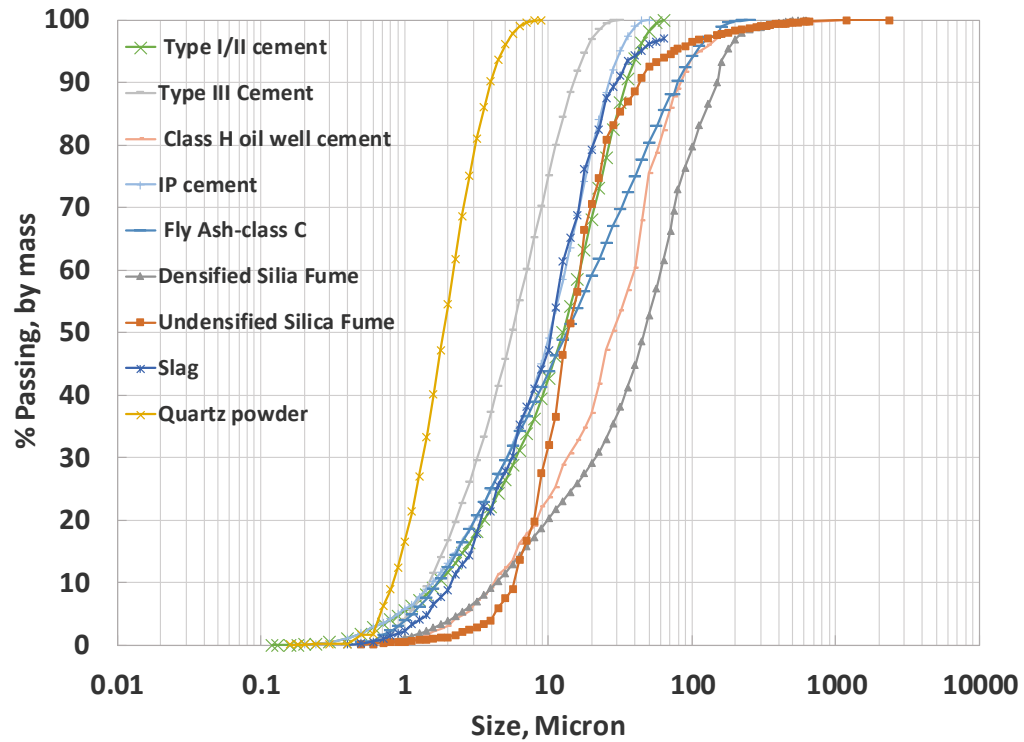


Figure 3.1. Particle size distribution of cement and various types of SCMs

It was observed that, because silica fume has a very fine particle size and strong surface charge, the particles of silica fume were agglomerated, showing a coarser particle size distribution in the densified silica fume. A portion of the agglomerates was expected to be dispersed after mixing. Thus, undensified silica fume was used in the analysis of the overall particle size distribution because it was believed that it better represented the gradation of the material in the UHPC mix. Note that, while a portion of the agglomerates was expected to be dispersed, a substantial amount still could remain in the mixture (Diamond and Sahu, 2006).

3.2.2 Aggregate

To ensure economically feasible UHPC mixes, the main aggregate used in this concrete mixture was silica sand that was available locally and had a maximum size of No. 10 (No. 10 sand). Three other aggregates, i.e., a commercially available fine silica sand (F75), a local limestone sand (Unical L), and local river sand also were used to evaluate the feasibility of further improving the design of the mix through optimization of the aggregate gradation. According to ASTM C136 (ASTM, 2014), sieve analyses were performed to obtain the gradation, and Figure 3. shows the gradation curves of the four aggregates.

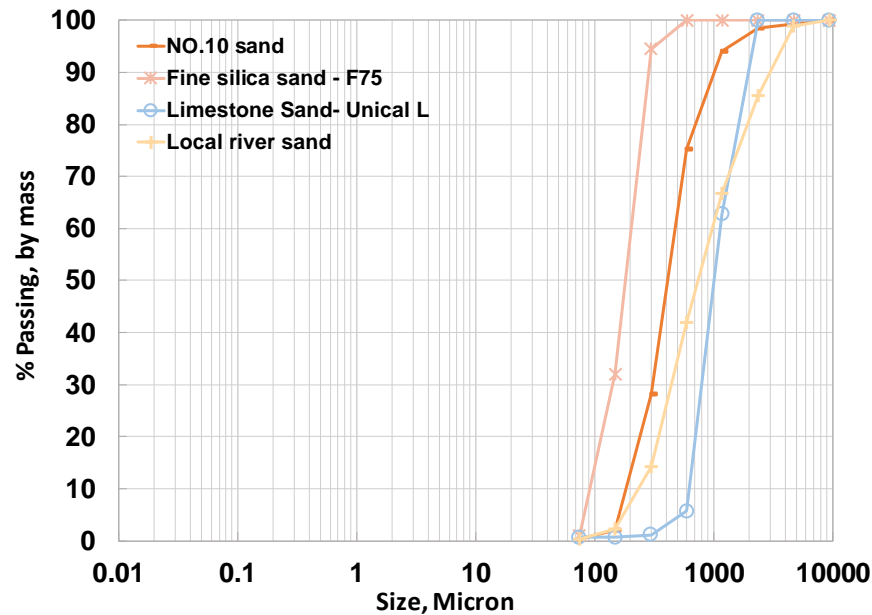


Figure 3.2. Particle size distribution of aggregates

3.2.3 Chemical admixtures

Due to the very low w/b and high flowability requirements, HRWR is important to ensure the success of the UHPC development. A modified polycarboxylate based, a polycarboxylate based that met ASTM C494 (ASTM, 2017) Type A and F and a polycarboxylate based that met ASTM C494 (ASTM, 2017) and ASTM C1017 (ASTM, 2013) Type I admixtures were used in this study. In addition, for preliminary mixes, two other polycarboxylate based admixtures that claimed, respectively, efficiency in dispersing powder materials and high early age strength were used. Also, a workability-retaining admixture was used in specific mixtures to reduce the workability loss.

3.2.4 Fibers

Figure 3.3 shows the four different types of fibers that were used in the study, i.e., a straight stainless steel micro-fiber (SS), two twisted steel fibers (TS13 and TS25), and a synthetic glass (SG) fiber.

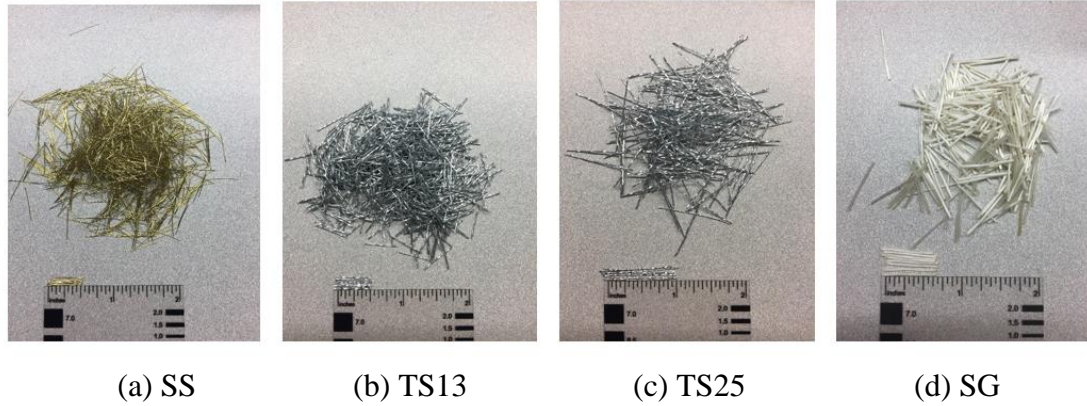


Figure 3.3. Fibers used in the study.

Table 3.2 provides the details of the physical and mechanical characteristics of the four fibers.

Table 3.2. Physical and mechanical properties of fibers

| | SS | TS13 | TS25 | SG |
|-----------------------------|--------|--------|--------|-------|
| Specific Gravity | 7.800 | 7.800 | 7.800 | 2.000 |
| Length (in) | 0.510 | 0.510 | 0.980 | 0.750 |
| Diameter (in) | 0.078 | 0.020 | 0.020 | 0.020 |
| Modulus of Elasticity (ksi) | 29,000 | 29,000 | 29,000 | 6,092 |
| Tensile Strength (ksi) | 399 | 247 | 247 | 247 |

1 in = 25.4 mm

1 ksi = 6.89 MPa

3.3 Test Methods

3.3.1 Fresh concrete

The properties of fresh UHPC normally are determined using the flow table test, which consists of filling a small cone-shaped mold atop a standard flow table, raising the mold from the mixture, and measuring the spread of the concrete. Figure 3.4 shows the standard flow table with a diameter of 10 in (254 mm), as specified in ASTM C230 (ASTM, 2014), that was used in the study.



Figure 3.4. Flow table

The test was conducted following ASTM C1856 (ASTM, 2017), and it consisted of filling the cone mold with UHPC without tamping, followed by lifting the mold, waiting $2 \text{ min} \pm 5 \text{ sec}$, and measuring the diameter. The average of the maximum and minimum diameters measured was reported as the flow value.

3.3.2 Hardened concrete

The compressive strength test was performed for all of the UHPC mixtures according to ASTM C1856 (ASTM, 2017) at 4, 14, and 28 days. The measurements of the cylindrical specimens used in the test were diameters of 3 in (76.2 mm) and lengths of 6 in (152.4 mm). The concrete was placed into the plastic molds as one single layer, and no consolidation was applied during the preparation of the specimens. After 24 hours, the specimens were removed from the molds and cured in saturated lime water at 73 °F (23 °C) until the tests were performed. Prior to the compressive strength test, a grinding machine was used to grind the ends of all of the specimens (Figure 3.5 (a)). The cylinders were tested using a 400-kip (1779-KN) capacity Forney compression machine,

as shown in Figure 3.5(b), with an applied loading rate of 1015 ± 49 lb/s (4559 ± 218 N/s).



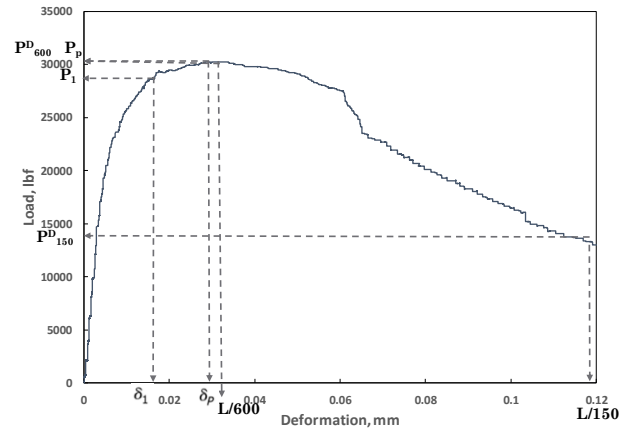
(a) Grinding machine (b) Compressive machine

Figure 3.5. Machine used for mechanical property testing.

The flexural strength test was conducted as directed by ASTM C1609 (ASTM, 2012). Each mix had two 6 in (152 mm) by 6 in (152 mm) cross-sections and a 20 in (508 mm) beam cast with one layer and no consolidation. The test was conducted using a Tinius Olsen Universal Testing Machine that has a capacity of 200 Kips (889 KN). The load rate applied was 0.0015 to 0.004 in/min (0.038 to 0.102 mm/min) up to the net deflection and 0.002 to 0.012 in/min (0.051 to 0.305 mm/min) beyond the net deflection. Two linear variable differential transformers (LVDTs), placed on the two lateral faces of the beam, were used to measure the deflection of the specimen, and the average of the displacements measured by the two LVDT's was reported. Figure 3.6(a) shows the test set up with the LVDTs attached to the specimen. Figure 3.(b) shows an example of the test results.



(a) Test setup



(b) Example of results

Figure 3.6. Flexural strength test setup and typical results.

3.4 Mixture development

3.4.1 Experimental approach

In this study, the UHPC design was developed based on a systematic plan that was divided into multiple stages. Stage 1 determined the aggregate type and combination. Stage 2 was the screening stage to determine the appropriate fiber, HRWR, and w/b to be used for the study. In Stage 3, the impact of the types of cement, the types and contents of the SCMs, and the total content of the binder on the performance of the UHPC were studied. Figure 3.7 shows the sequence of the stages and the parameters that were analyzed in each stage to design the UHPC.

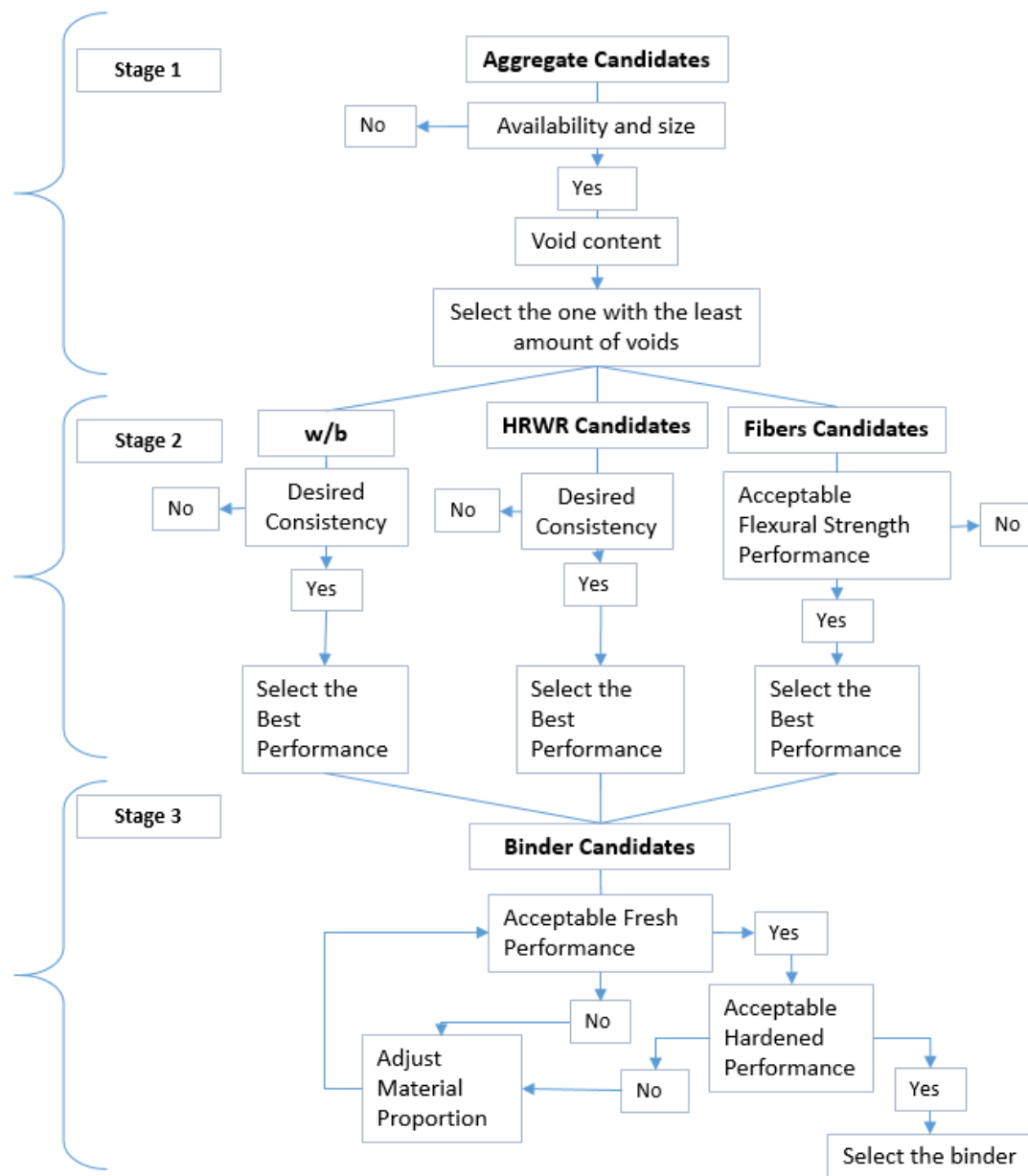


Figure 3.7. Flow chart of mixture development.

Since it generally is believed that the mixer and the volume of material mixed can influence the mixing procedure and, consequently, the performance of the UHPC, an

additional stage (stage 4) was used to evaluate the impact of the mixers on the performance of the fresh and hardened UHPC.

For this study, the identification of the mix began with the type of cement, and this was followed by a letter that refers to the other type of binder, a number that indicates the percentage of the additional binder based on its volume fraction of all of the binder, and the last letter refers to the fiber that was used. To identify the cement, IP stands for IP cement, I/II stands for Type I/II cement, III stands for Type III cement, and OWH stands for class H oil well cement. For the type of binder, SF stands for silica fume, FA stands for Class C fly ash, S stands for slag, and QP stands for quartz powder. The following letters indicate the types of fibers that were used, i.e., SS (straight steel fiber), TS13 and TS25 (the two twisted steel fibers), and SG (synthetic fiber glass fiber). As an example, I/II:SF19:FA16:S0:QP0:SS uses Type I/II cement, 19% silica fume, and 16% fly ash in the total volume of the binder. The mix does not contain slag or quartz powder, and the fiber used in this mix was a straight steel fiber. The designs of the mixes presented in this chapter are presented in pcy and the aggregate is in SSD condition.

3.4.1.1 Selection of the aggregate, fiber, HRWR, and w/b

a) Aggregate

As mentioned earlier in this chapter, stage 1 of the experimental study was to select an appropriate aggregate for the development of UHPC. Aggregates account for the largest amount of the materials in the design. Therefore, to ensure cost effectiveness, aggregates candidates were selected based on their availability. A preliminary study showed that as the particle size of the river sand and limestone sand are significantly larger than binder materials particles, which lead to a low packing due to the large gap in

particle size. The finding is consistent with the information as shown in Chapter 2, that aggregates with finer particles are desirable in the UHPC matrix. Also, a preliminary study also demonstrated that the resulting strength of concrete made with river sand and limestone could not achieve sufficient strength for UHPC development. The focus on aggregate selection was therefore focused only on the No. 10 sand and fine silica sand. A void content test per ASTM C1252 (ASTM, 2006) of different aggregates and aggregate combinations was performed in order to identify the aggregates matrix that provides the least amount of voids. The test was performed on of No.10 sand and fine silica sand (F75) separately and combined when a portion of No.10 sand was replaced by fine silica sand (F75). A compacted voids test was conducted as suggested by De Larrard (1999) to account for the high fineness of the materials. Since the surface charge of the fine particles may result in repulsion forces among them, compaction can minimize the interaction force between the fine particles and provide a more accurate value of the voids. The compacted void test consists of filling a 0.25 ft³ (0.03 m³) container with the aggregate or combination of aggregates and vibrating them for 1 minute using a vibrating table. During the vibration, an external pressure of 1.45 psi (10 KPa) was applied to the specimens. The volume occupied by the aggregate was calculated by measuring the height of the aggregate inside the container after vibration and multiplying the height the area of the circular bottom face of the container. The percentage of voids was calculated by Equation 3.1.

$$Void\% = \frac{(SG \times UW_{water}) - \frac{W}{V}}{(SG \times UW_{water})}$$

Equation 3.1

where SG is the specific gravity of the aggregate or combination of aggregates, UW_{water} is the unit weight of the water, W is the mass of the aggregate, and V is the volume occupied by the aggregate. The specific gravity of the combination of aggregates was calculated using Equation 3.2.

$$SG_{comb} = \frac{1}{\left(\frac{P_1}{SG_1} + \frac{P_2}{SG_2}\right)} \quad \text{Equation 3.2}$$

where P_1 and P_2 are the percentages of aggregate 1 and aggregate 2, respectively, and SG_1 and SG_2 are the specific gravity of aggregate 1 and aggregate 2, respectively.

Stage 2 can be divided further into three series, i.e., series 1 to determine the appropriate fiber, series 2 (HRWR), and series 3 (w/b).

b) Fibers

Stage 2 of series 1 consists of the determination of the most effective type of fiber to be used. Specimens were prepared with a representative design that had the same volume fraction (2%) but different types of fibers. The type that provided the highest flexural strength and toughness was selected. As mentioned earlier, four types of fibers were studied, i.e., a straight stainless steel fiber (SS), two twisted steel fibers (TS13 and TS25), and a synthetic glass fiber (SG). The performance of the UHPC mixtures was evaluated with a flexural load applied. Table 3.3 shows the design of mixes that were prepared with different fibers. A commercial product using 2% by volume of straight steel fibers also was tested for comparison.

Table 3.3. Mix design of mixes prepared with different fibers

| Mix ID | Cement | Silica Fume | Fly ash | Slag | Quartz powder | Water | Sand | Fiber | HRWR | w/b |
|----------------------------|--------|-------------|---------|------|---------------|-------|------|-------|------|-------|
| I/II: SF8:FA22:S0:QP0:SS | 1076 | 87 | 294 | 0 | 0 | 250 | 2123 | 251 | 48 | 0.194 |
| I/II: SF8:FA22:S0:QP0:TS13 | 1074 | 87 | 293 | 0 | 0 | 244 | 2107 | 229 | 48 | 0.191 |
| I/II: SF8:FA22:S0:QP0:TS25 | 1080 | 87 | 295 | 0 | 0 | 243 | 2134 | 249 | 48 | 0.189 |
| I/II: SF8:FA22:S0:QP0:SG | 1070 | 86 | 292 | 0 | 0 | 243 | 2109 | 64 | 47 | 0.191 |

Note: All units are in pcy (1 pcy = 0.59 Kg/m³)

c) High Range Water Reducer (HRWR)

Since the significantly low w/b of UHPC makes the use of HRWR essential, stage 2 series 2 includes mixes with a representative design but different HRWRs were prepared to identify the most effective HRWR for UHPC. The admixtures are introduced in the mix to provide sufficient flowability to ensure good consistency and compaction during casting. Therefore, HRWR should be selected to provide concrete with the desired performance at the low w/b used in the design.

The HRWR that provided the desired UHPC consistency with the least amount of water was selected. Note that two polycarboxylate based HRWRs that claimed, respectively, efficiency in dispersing powder materials and high early age strength were used in preliminary mixes and were not selected for further study due to their substantially-low workability. Table 3.4 shows the mix design of stage 2 series 2 mixes with different HRWRs. The mix identification has a number (1, 2, or 3) added after “HRWR,” and the numbers indicate the three types of HRWRs, i.e., HRWR1 the modified polycarboxylate based, HRWR2 the polycarboxylate based that met ASTM

C494 (ASTM, 2017) Type A and F and HRWR3 the polycarboxylate based that met ASTM C494 (ASTM, 2017) and ASTM C1017 (ASTM, 2013) Type I.

Table 3.4. Mix design of mixes prepared with different HRWRs

| Mix ID | Cement | Silica Fume | Fly ash | Slag | Quartz powder | Water | Sand | Fiber | HRWR | w/b |
|--------------------------------|--------|-------------|---------|------|---------------|-------|------|-------|------|-------|
| I/II:SF11:FA0:S34:QP0:SS:HRWR1 | 883 | 117 | 0 | 427 | 0 | 239 | 2129 | 266 | 51 | 0.192 |
| I/II:SF11:FA0:S34:QP0:SS:HRWR2 | 880 | 117 | 0 | 426 | 0 | 238 | 2124 | 266 | 50 | 0.192 |
| I/II:SF11:FA0:S34:QP0:SS:HRWR3 | 880 | 117 | 0 | 426 | 0 | 238 | 2124 | 266 | 50 | 0.192 |

Note: All units are in pcy (1 pcy = 0.59 Kg/m³)

d) Water-to-binder ratio (w/b)

Stage 2 series 3 selected the w/b to be used in the mixes. According to the literature review presented in Chapter 2, the reported w/b values of UHPC mixtures can be as low as 0.16, and they range mostly between 0.16 and 0.19. While a low w/b value could result in high packing density, it also indicates the risk of insufficient water for the hydration of the cement. To evaluate the impact of w/b, we prepared mixes with their w/b values reduced from approximately 0.190 to approximately 0.170. For mixes in stage 2 series 3, as shown in Table 3.5, an additional parameter (WB), which represents the value of w/b rounded to two decimal points, was added in the identification of the mix.

Table 3.5. Mix design of mixes prepared with different w/b values

| Mix ID | Cement | Silica Fume | Fly ash | Slag | Quartz powder | Water | Sand | Fiber | HRWR | w/b |
|-------------------------------|--------|-------------|---------|------|---------------|-------|------|-------|------|-------|
| I/II:SF11:FA22:S0:QP0:SS:WB19 | 1098 | 123 | 308 | 0 | 0 | 252 | 1959 | 251 | 54 | 0.190 |
| I/II:SF20:FA22:S0:QP0:SS:WB19 | 1167 | 292 | 368 | 0 | 0 | 302 | 1587 | 253 | 64 | 0.190 |
| I/II:SF30:FA22:S0:QP0:SS:WB19 | 1016 | 437 | 367 | 0 | 0 | 301 | 1580 | 252 | 64 | 0.190 |
| I/II:SF11:FA22:S0:QP0:SS:WB17 | 1155 | 129 | 324 | 0 | 0 | 230 | 2060 | 264 | 56 | 0.168 |
| I/II:SF20:FA22:S0:QP0:SS:WB17 | 1202 | 301 | 380 | 0 | 0 | 270 | 1635 | 261 | 66 | 0.168 |
| I/II:SF30:FA22:S0:QP0:SS:WB17 | 1020 | 438 | 368 | 0 | 0 | 262 | 1587 | 253 | 64 | 0.168 |

Note: All units are in pcy (1 pcy = 0.59 Kg/m³)

3.4.1.2 Selection of the Binder

Stage 3 elevates the performance of the UHPC mixes that were developed with different types and contents of binders. As the impact of binder composition (cement and SCMs type, and relative content), as well as the total binder content on particle packing, workability, and hydration of UHPC are often interrelated, there is no practical way to obtain the optimum binder composition and content directly. The focus of this study is therefore to identify the best binder composition and content based on the evaluation of UHPC performance with the adjustment of the component at a time. The stage consisted of ternary binder mixes using cement and other types and quantities of binders. The mixes can be divided further into 5 series, with each series focused on only one parameter. The investigation involved the evaluation of the performances of fresh and hardened concrete. The fresh test was the flow table test, and the hardened test was the compressive strength test. For the binder type to be selected for further investigation, the concrete had to have a promising flow value greater than 6 in (203 mm) and a promising 28-day compressive strength higher than 10 ksi (69 MPa). The modified A&A particle packing theory model was used as the initial guide for deciding the proportions of the

materials. The total binder content was increased further, and the performance was analyzed.

Mixes prepared for stage 3 had cement and types of SCMs evaluated while other parameters, including fiber, aggregate, HRWR, and w/b, remained the same. Figure 3.8 shows a summary of the cement and SCMs materials and the quantities tested. The amounts presented for each of the SCMs is in the percentage of volume out of the whole binder content.

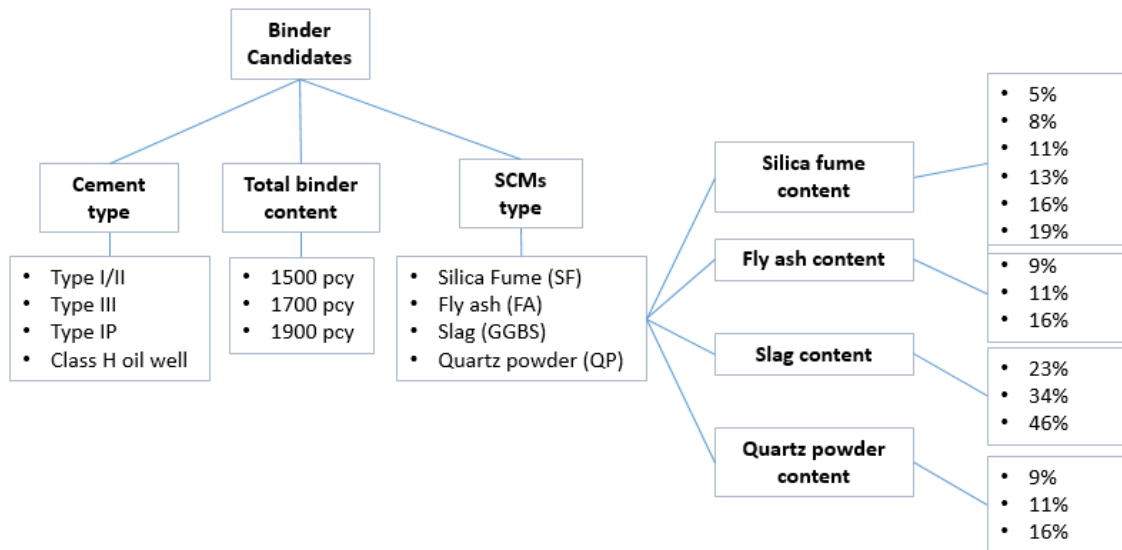


Figure 3.8. Cement and SCMs types and quantities used in stage 3 study

This stage was divided further into various series. Series 1 evaluated different types of cement to be used in the UHPC mixes. Series 2, series 3, series 4, and series 5 investigated different silica fume content, fly ash content, slag content, and quartz powder content, respectively. The impacts of the types and quantities of binders were analyzed within each series and between the series.

a) Impact of the type of cement

As mentioned before, four types of cement were investigated in series 1 due to its importance in the design of UHPC. In addition to Type I /II cement, Type III was included due to its high fineness, which could be helpful for strength at an early age. A locally-available Type IP cement that consists of 25% Class F fly ash and 75% Type I cement also was included. Type IP cement also has slightly higher fineness than Type I/II cement. Finally, a Class H oil well cement was used due to its lower fineness, which can improve the particle packing of UHPC and low C_3A content. Table 3.6 shows the design of the mixes that were prepared with different types of cement.

Table 3.6. Mix design prepared with different types of cement

| Mix ID | Cement | Silica Fume | Fly ash | Slag | Quartz powder | Water | Sand | Fiber | HRWR | Work. Retaining | w/b |
|---------------------------|--------|-------------|---------|------|---------------|-------|------|-------|------|-----------------|-------|
| I/II: SF11:FA0:S34:QP0:SS | 906 | 120 | 0 | 438 | 0 | 245 | 2185 | 273 | 52 | 0 | 0.192 |
| IP: SF11:FA0:S34:QP0:SS | 902 | 120 | 0 | 436 | 0 | 244 | 2176 | 276 | 51 | 0 | 0.192 |
| OWH: SF11:FA0:S34:QP0:SS | 921 | 123 | 0 | 446 | 0 | 229 | 2222 | 275 | 52 | 0 | 0.178 |
| III: SF11:FA22:S0:QP0:SS | 1119 | 125 | 314 | 0 | 0 | 240 | 1687 | 265 | 54 | 21 | 0.189 |
| I/II: SF11:FA22:S0:QP0:SS | 986 | 110 | 277 | 0 | 0 | 229 | 2004 | 261 | 51 | 0 | 0.192 |

Note: All units are in pcy (1 pcy = 0.59 Kg/m³)

b) Impact of silica fume

Series 2 evaluated the impact of the content of silica fume in the UHPC mixes. Because of its very fine particle size, it is believed that silica fume helps to provide denser particle packing (Holland, 2005), which, in turn, leads to increased strength. However, it also can have a negative affect on flowability due to its fineness. Low flowability can result in the formation of extensive entrapped air during the casting process, which will reduce the compressive strength. Therefore, the amount of silica

fume should be well controlled. Thus, in series 2, the content of silica fume in UHPC was increased gradually from 5% to 19% by volume of the binder and the properties of the UHPC were evaluated.

In order to compare the impact of densified and undensified silica fume on the fresh and hardened properties of UHPC, two mixes with 11% of undensified silica fume were prepared, one with 22% fly ash, and the other with 46% slag (percentage by volume of binder). Table 3.7 presents the designs of the series 2 mixes.

Table 3.7. Mix design of the mixes prepared with different contents of silica fume

| Mix ID | Cement | Silica Fume | Fly ash | Slag | Quartz powder | Water | Sand | Fiber | HRWR | w/b |
|--------------------------------------|--------|-------------|---------|------|---------------|-------|------|-------|------|-------|
| I/II: SF5:FA22:S0:QP0:SS | 1108 | 58 | 295 | 0 | 0 | 247 | 2130 | 251 | 46 | 0.192 |
| I/II: SF8:FA22:S0:QP0:SS | 1076 | 87 | 294 | 0 | 0 | 250 | 2123 | 251 | 48 | 0.194 |
| I/II: SF11:FA22:S0:QP0:SS | 1049 | 117 | 294 | 0 | 0 | 247 | 2132 | 251 | 51 | 0.194 |
| I/II: SF13:FA22:S0:QP0:SS | 997 | 143 | 287 | 0 | 0 | 233 | 2081 | 246 | 46 | 0.186 |
| I/II: SF16:FA22:S0:QP0:SS | 987 | 175 | 293 | 0 | 0 | 236 | 2119 | 252 | 63 | 0.192 |
| I/II: SF19:FA22:S0:QP0:SS | 928 | 215 | 288 | 0 | 0 | 230 | 2098 | 250 | 66 | 0.193 |
| I/II: UndensifiedSF11:FA22:S0:QP0:SS | 1050 | 118 | 295 | 0 | 0 | 244 | 2135 | 251 | 51.3 | 0.192 |
| I/II: UndensifiedSF11:FA0:S46:QP0:SS | 691 | 118 | 0 | 586 | 0 | 234 | 2138 | 266 | 50.7 | 0.192 |

Note: All units are in pcy (1 pcy = 0.59 Kg/m³)

c) Impact of fly ash

Series 3 evaluated the effect of fly ash in the UHPC mixes. Fly ash particles are spherical, which helps the concrete flow. Moreover, the pozzolanic reaction results in a gain in strength. However, because fly ash is an industrial byproduct, and coal-burning power plants have undergone some major changes during the last decade due to changes in regulations made by the Environmental Protection Agency (EPA), the batch-to-batch

variation of fly ash products tends to be high, which sometimes causes the issue of inconsistency.

Table 3.8 shows a series of mixes that were prepared with the fly ash content increasing gradually from 9% to 22% by volume of total binder.

Table 3.8. Mix design of mixes prepared with fly ash

| Mix ID | Cement | Silica Fume | Fly ash | Slag | Quartz powder | Water | Sand | Fiber | HRWR | w/b |
|---------------------------|--------|-------------|---------|------|---------------|-------|------|-------|------|-------|
| I/II: SF19:FA22:S0:QP0:SS | 928 | 215 | 288 | 0 | 0 | 230 | 2098 | 250 | 66 | 0.193 |
| I/II: SF19:FA16:S0:QP0:SS | 1086 | 233 | 233 | 0 | 0 | 262 | 1988 | 257 | 48 | 0.191 |
| I/II: SF19:FA11:S0:QP0:SS | 1157 | 231 | 154 | 0 | 0 | 260 | 1977 | 256 | 54 | 0.193 |
| I/II: SF19:FA09:S0:QP0:SS | 1183 | 232 | 130 | 0 | 0 | 261 | 1980 | 256 | 54 | 0.193 |

Note: All units are in pcy (1 pcy = 0.59 Kg/m³)

d) Impact of slag

Although slag has rough, angular-shaped particles that might not necessarily improve the flow, it is a more reactive and consistent material than fly ash, and it potentially could result in better UHPC performance. Thus, series 4 consists of mixes that were prepared with the slag content increasing gradually from 23% to 46% by volume of binder. Table 3.9 presents the design of the mixes.

Table 3.9. Mix design of the mixes prepared with slag

| Mix ID | Cement | Silica Fume | Fly ash | Slag | Quartz powder | Water | Sand | Fiber | HRWR | w/b |
|---------------------------|--------|-------------|---------|------|---------------|-------|------|-------|------|-------|
| I/II: SF11:FA0:S23:QP0:SS | 1064 | 119 | 0 | 299 | 0 | 245 | 2164 | 255 | 52 | 0.190 |
| I/II: SF11:FA0:S34:QP0:SS | 906 | 120 | 0 | 438 | 0 | 245 | 2185 | 273 | 52 | 0.192 |
| I/II: SF11:FA0:S46:QP0:SS | 711 | 121 | 0 | 603 | 0 | 240 | 2200 | 274 | 52 | 0.192 |

Note: All units are in pcy (1 pcy = 0.59 Kg/m³)

e) Impact of quartz powder

Quartz powder is a very fine filler that can impact the overall particle packing. Series 5 mixes were prepared by replacing fly ash from mixes of series 3 with quartz powder. Then, the performance of UHPC was evaluated. Table 3.10 presents the design of series 4 mixes.

Table 3.10. Mix design of the mixes prepared with quartz powder

| Mix ID | Cement | Silica Fume | Fly ash | Slag | Quartz powder | Water | Sand | Fiber | HRWR | w/b |
|---------------------------|--------|-------------|---------|------|---------------|-------|------|-------|------|-------|
| I/II: SF19:FA0:S0:QP16:SS | 1075 | 230 | 0 | 0 | 230 | 259 | 1968 | 254 | 48 | 0.191 |
| I/II: SF19:FA0:S0:QP11:SS | 1159 | 232 | 0 | 0 | 155 | 261 | 1980 | 256 | 54 | 0.193 |
| I/II: SF19:FA0:S0:QP9:SS | 1202 | 236 | 0 | 0 | 132 | 265 | 2021 | 260 | 55 | 0.193 |

Note: All units are in pcy (1 pcy = 0.59 Kg/m³)

f) Impact of total binder content

Cement paste is necessary in the UHPC to fill the voids of the aggregate matrix and to coat the aggregate particles and fibers, thereby minimizing the friction between the aggregate and the fiber, especially when rigid fibers are used, since the particles tend to interact and often make the flow more difficult (Naaman and Wille, 2010). The paste used to coat particles and fibers is called excess paste. According to Hu (2005), since the paste is the only phase inside a concrete mixture that can provide flowability, the excess paste enhances the flowability due to the reduction of friction between the particles and the fibers.

As the content of binder increases, the excess paste is increased. Thus, it is essential to evaluate the impact of the total content of the binder on the performance of

the UHPC. Two groups of mixes with, IP, and class H oil well cement were prepared with a graduated increase of binder content from 1600 to 1900 pcy (949 to 1127 Kg/m³), respectively. Table 3.11 presents the design of the mixes prepared with different contents of binder. The same identification from the mixes presented before was used with the addition of the letter “B,” followed by the total binder content rounded to the nearest 50 pcy.

Table 3.11. Mix design of mixes prepared with different total binder contents

| Mix ID | Cement | Silica Fume | Fly ash | Slag | Quartz powder | Water | Sand | Fiber | HRWR | w/b |
|--------------------------------|--------|-------------|---------|------|---------------|-------|------|-------|------|-------|
| IP: SF11:FA0:S34:QP0:SS:B1500 | 902 | 120 | 0 | 436 | 0 | 244 | 2176 | 276 | 51 | 0.192 |
| IP: SF11:FA0:S34:QP0:SS:B1700 | 1065 | 141 | 0 | 516 | 0 | 288 | 1862 | 282 | 60 | 0.192 |
| IP: SF11:FA0:S34:QP0:SS:B1900 | 1182 | 157 | 0 | 573 | 0 | 319 | 1498 | 278 | 67 | 0.192 |
| OWH: SF11:FA0:S34:QP0:SS:B1500 | 921 | 123 | 0 | 446 | 0 | 229 | 2222 | 275 | 52 | 0.178 |
| OWH: SF11:FA0:S34:QP0:SS:B1700 | 1094 | 145 | 0 | 529 | 0 | 238 | 1913 | 276 | 62 | 0.159 |
| OWH: SF11:FA0:S34:QP0:SS:B1900 | 1281 | 171 | 0 | 621 | 0 | 278 | 1624 | 286 | 73 | 0.159 |

Note: All units are in pcy (1 pcy = 0.59 Kg/m³)

3.4.2 Particle packing theory

The intent of the particle packing theory is to reduce the porosity of the concrete matrix by filling the voids in larger particles with smaller particles. The optimum proportion of combined materials theoretically can be obtained by using the theoretical model. Generally, it is believed that an optimum particle packing will provide the best UHPC performance. The modified Andreasen and Andersen particle packing model was used in this study, and an optimum curve was created using Equation 2.2 with a q value of 0.23, based on the previous study by Yu et al. (2015).

3.5 Mixing

3.5.1 Impact of the mixer

Sufficient mixing energy is essential to properly disperse UHPC materials, especially the fine materials. Since HRWR is used in UHPC, a longer mixing time compared to conventional concrete generally is necessary to produce concrete with the desired consistency, which is determined by visual examination of the fresh material. In order to evaluate the impact of the mixer and mixing energy on the performance of UHPC, stage 4 consists of selected mixes from the previous stages that were prepared using three different mixers with the different batch volumes, i.e., small, medium, and large batches. The volumes of the small, medium, and large batches were 0.16 ft³ (0.0045 m³), 1.25 ft³ (0.035 m³), and 2.0 ft³ (0.06 m³), respectively. Table 3.12 shows the mix design of the selected mixtures. Mixes from stage 2, series 1, I/II were SF8:FA22:S0:QP0:SS, I/II: SF8:FA22:S0:QP0:TS13, I/II: SF8:FA22:S0:QP0:TS25 and I/II: SF8:FA22:S0:QP0:SG, and they were mixed in a small batch volume and a large batch volume. Two selected mixtures from stage 3 series 5, I/II: SF11:FA0:S23:QP0:SS and I/II: SF11:FA0:S46:QP0:SS, were mixed in the small batch volume and the medium batch volume. Note that, for some of the mixes, the water had to be adjusted slightly to achieve the desired UHPC consistency based on visual examination.

Table 3.12. Mix design of mixes using different mixers

| Mix ID | Cement | Silica Fume | Fly ash | Slag | Quartz powder | Water | Sand | Fiber | HRWR | Work. Retaining | w/b |
|----------------------------|--------|-------------|---------|------|---------------|-------|------|-------|------|-----------------|-------|
| I/II: SF8:FA22:S0:QP0:SS | 1074 | 87 | 293 | 0 | 0 | 245 | 2110 | 247 | 48 | 0 | 0.191 |
| I/II: SF8:FA22:S0:QP0:TS13 | 1043 | 84 | 285 | 0 | 0 | 236 | 2060 | 240 | 46 | 0 | 0.190 |
| I/II: SF8:FA22:S0:QP0:TS25 | 1080 | 87 | 295 | 0 | 0 | 245 | 2131 | 249 | 48 | 0 | 0.191 |
| I/II: SF8:FA22:S0:QP0:SG | 1051 | 85 | 287 | 0 | 0 | 235 | 2065 | 63 | 47 | 0 | 0.188 |
| I/II: SF11:FA0:S23:QP0:SS | 1044 | 117 | 0 | 293 | 0 | 268 | 2123 | 266 | 34 | 17 | 0.209 |
| I/II: SF11:FA0:S46:QP0:SS | 691 | 118 | 0 | 586 | 0 | 222 | 2120 | 266 | 48.9 | 16.3 | 0.192 |

Note: All units are in pcy (1 pcy = 0.59 Kg/m³)

3.5.2 Mixing procedures

One other important factor that impacts the performance of UHPC is the mixing procedure. Because of the very fine particle sizes, the elimination of the coarse aggregate, and the very low w/b, higher mixing energy generally is needed, which results in a longer mixing time than conventional concrete to ensure good distribution of all of the particles (Wille et al., 2011). Since UHPC's ingredients are composed of very fine particles and they are likely to agglomerate and form chunks, mixing these particles in dry condition is very important to reduce the shear force required to break the pieces.

The process of mixing UHPC can be very peculiar and specific for the different mixers used and the volumes of the materials that are being mixed. In this study, three different mixers were used, and the results were compared. A 20-qt capacity Vollrath benchtop mixer (0.5 HP) with three different speeds was used for all the batches with 0.16 ft³ (0.0045 m³) of UHPC (small batches). For comparison, selected mixes also were prepared using a 3 ft³ (0.085 m³) capacity Imer Mortarman 120+ mixer (2 HP) with batch sizes of approximately 1.25 ft³ (0.035 m³) (medium batch), and a 16 ft³ (0.45 m³) capacity Imer Mortarman 750 mixer (5 HP) with batch sizes of approximately 2 ft³ (0.06 m³)

(large batches). The mixing process generally can be separated into three main steps, i.e., (1) mix the dry components and air dry all of the aggregates to a moisture content of approximately 0.1% prior to mixing; (2) add water and superplasticizer; (3) add the fibers. Generally, the final product of UHPC should have a flowable and viscous consistency, as determined by visual examination of the fresh material. Because of the different paddle configurations, dimensions, and speed, the mixing time will differ depending on the mixer and the volume of the batch.

The mixing procedures used in this study were developed based on the literature (Naaman and Wille, 2012; Graybeal and Hartmann, 2003; Alkaysi and El-Tawil, 2015) and adjusted based on consistency changes during the mixing of the trial batch. Figure 3.9 shows the procedures for the three different mixers and batch sizes that were used in this study.

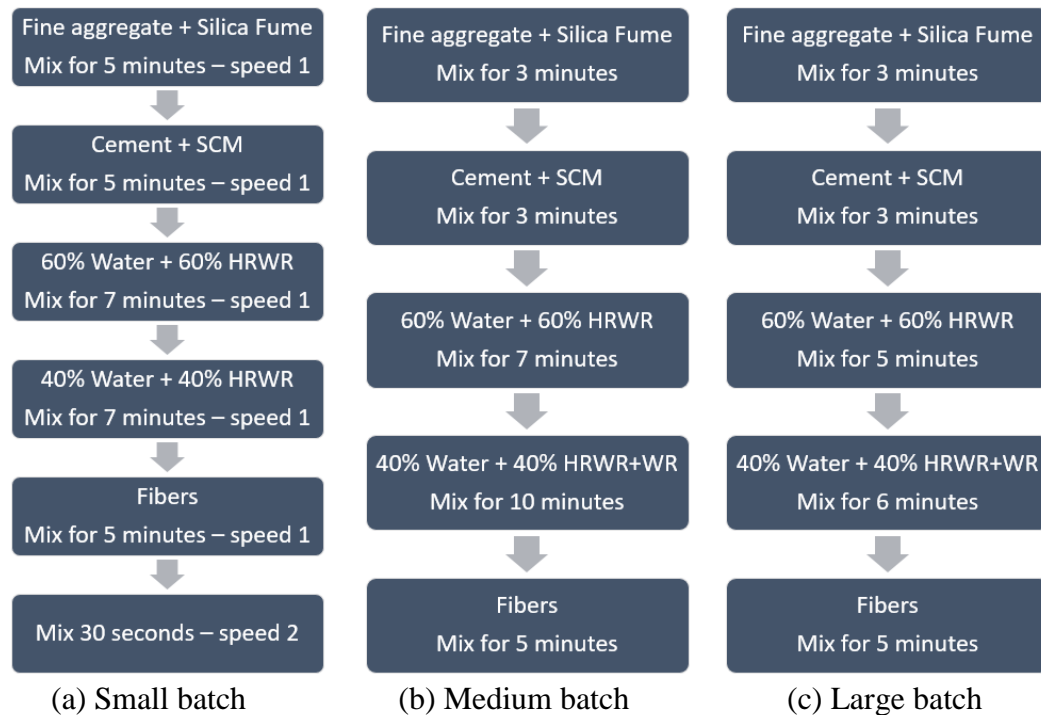
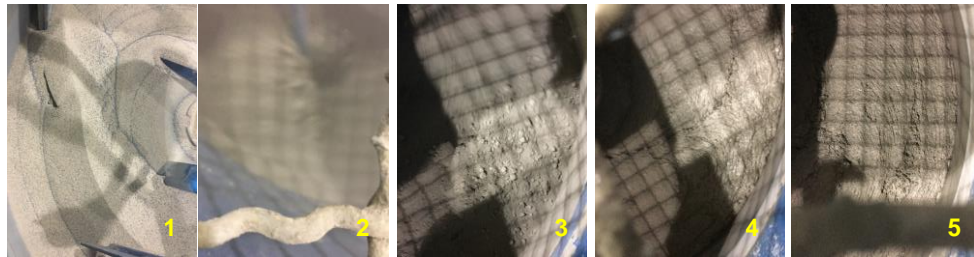


Figure 3.9. Flow charts of the batching and mixing procedures for different sizes of batches

Figure 3.10 shows the appearance of mixtures at the different mixing stages described before in the flow chart for the small mixers (top figures) and large mixers (bottom figures). In Figure 3.10, photograph (1) is after mixing the aggregate and the silica fume; photograph (2) is after mixing cement and fly ash; photograph (3) is after mixing the first portion of the premixed liquid; photograph (4) is after mixing the second portion of the premixed liquid; photograph (5) is the final product after the fibers were loaded.



(a) Small batch



(b) Large batch

Figure 3. 10. Comparison of changes in the mixers and the consistency during mixing:

3.6 Summary

This chapter presented the details of the experimental study to investigate the impact of different materials in the UHPC mixes. The performances of the mixes were evaluated with different types of aggregates, fiber, HRWR, w/b, cement types, SCM types and quantities, and different total binder quantity and different mixers.

The chapter also includes the tests methods and procedures used, the development methodology associated with the design of the mixtures, and the performance of concrete prepared with the three different mixers and mixing procedures.

CHAPTER 4: RESULTS AND DISCUSSION

4.1 Introduction

Chapter 4 presents the fresh and hardened properties of the developed UHPC. First, the results of the void content test conducted on the different aggregate candidates are presented. Then, the results of flexural strength conducted in the UHPC with different fibers are shown, along with the flow and compressive strength of the mixes with different HRWR, w/b, types of cement, types and content of SCMs, and total binder content. Also, the effects of different mixers in the fresh and hardened UHPC are presented. Also, the results and the selection of materials to be used in the UHPC mixes, as well as the results of the particle packing of representative mixes are discussed.

4.2 Results and discussion of aggregate, fibers, HRWR, and w/b selection

4.2.1 Aggregate

In stage 1, No.10 sand and fine silica sand (F75) were tested to determine the content of voids in the uncompacted and compacted methods, and Figure 4.1 shows the results.

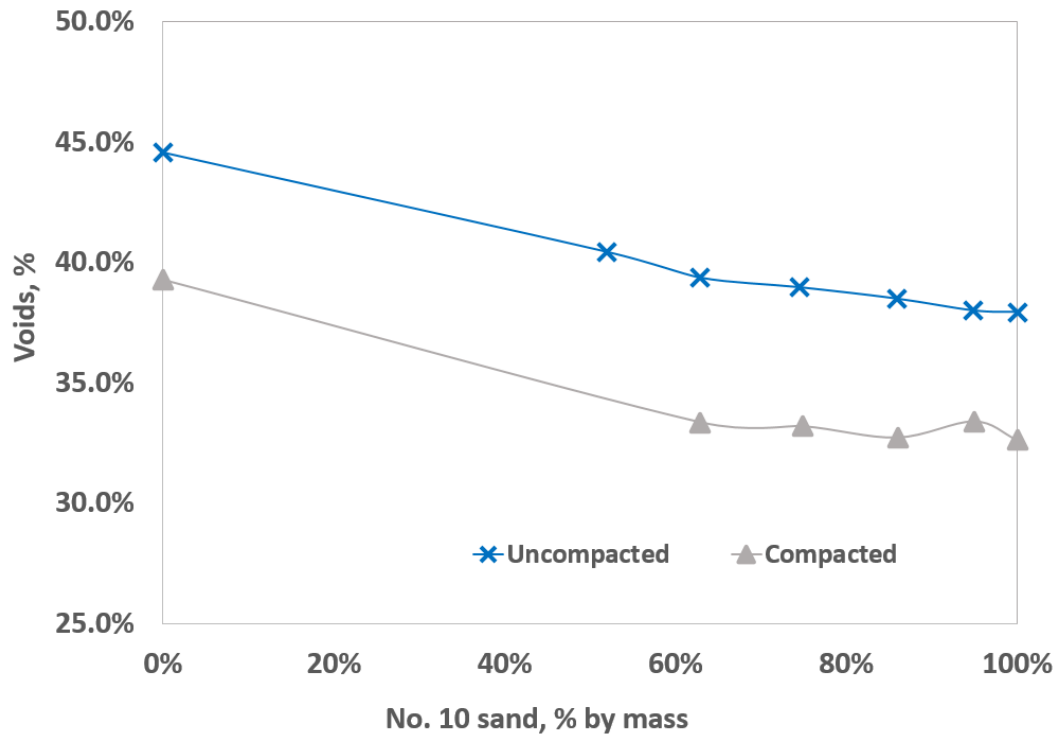


Figure 4.1. Uncompacted and compacted voids of aggregates in the No. 10 sand matrix

Figure 4.1 shows that, when fine silica sand (F75) was introduced into the No.10 sand matrix, the particle packing was disturbed slightly, resulting in an increase in the percentage of the uncompacted and compacted voids in the matrix. Figure 4.1 also shows that and F75, when analyzed individually, had higher void contents than No. 10 sand. The results indicate that a single-aggregate system should be selected, i.e., No. 10 sand in the UHPC mixes, considering that it is locally available and that the least amount of voids is desirable to achieve a denser structure in the UHPC matrix. Local river sand and limestone sand (Unical L) were not selected for further investigation due to their coarser particles when compared to No.10 sand and fine silica sand (F75). Based on the literature, finer particles are desirable to get a denser internal UHPC structure. Also,

preliminary mixes were conducted with local river sand and results indicated that it cannot provide UHPC with sufficient strength.

4.2.2 Fibers

As mentioned in Chapter 3, stage 2 series 1 includes the investigation of the impact of four types of fibers (SS, TS13, TS25, and SG) on the flexural behavior of UHPC. Figure 4.2 shows the load-displacement relationship of mixes of a commercial UHPC prepared with the four different types of fibers at 28 days.

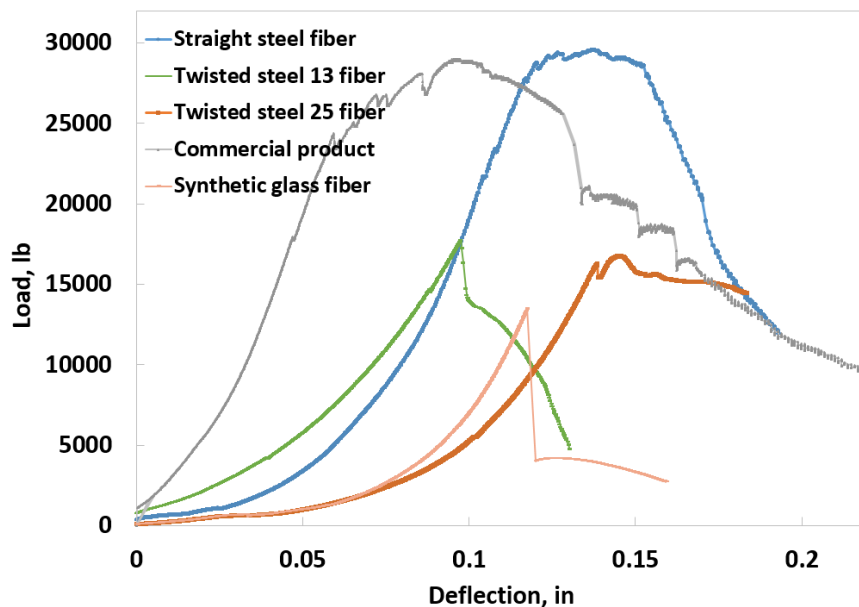


Figure 4.2. Load-displacement relationship of the flexural behavior of UHPC with different types of fibers

The flexural strength data at 28 days shown in Figure 4.2 suggests the selection of micro straight steel (SS) fibers due to their higher modulus of rupture and higher toughness compared to the other three types of fibers that were tested. The mix with SS fibers provided results that were comparable to the commercial UHPC product. Note that

the curve for the mix with synthetic glass fibers was for a 4-day concrete test, but no major changes were expected between the 4-day and 28-day tests.

4.2.3 High Range Water Reducer (HRWR)

Stage 2 series 2 consisted of mixtures with three different HRWRs. HRWR #1 was chosen to be used in the UHPC mixes since it provided a flowable mix with about 9.6 inches of flow, 0.19 w/b, and reasonable compressive strength, i.e., $f'_{c,4}$ at about 13,000 psi and $f'_{c,28}$ at about 17,200 psi. The other two HRWRs (#2 and #3) did not provide the desired consistency with 0.19 w/b, as determined by visual examination of the mixtures at the fresh stage. Figures 4.3a and 4.3b show examples of the UHPC with the desired consistency and poor consistency, respectively. Note that for clearer demonstration, the pictures were taken prior to fiber be added into the mixture



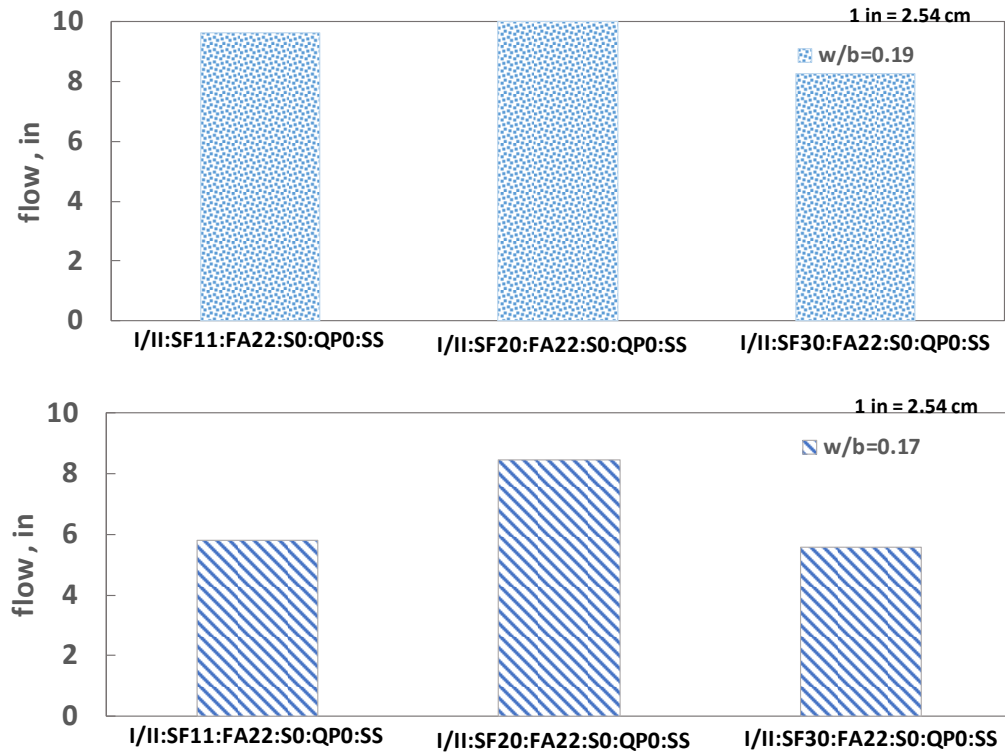
(a) Desired consistency

(b) Unacceptable consistency

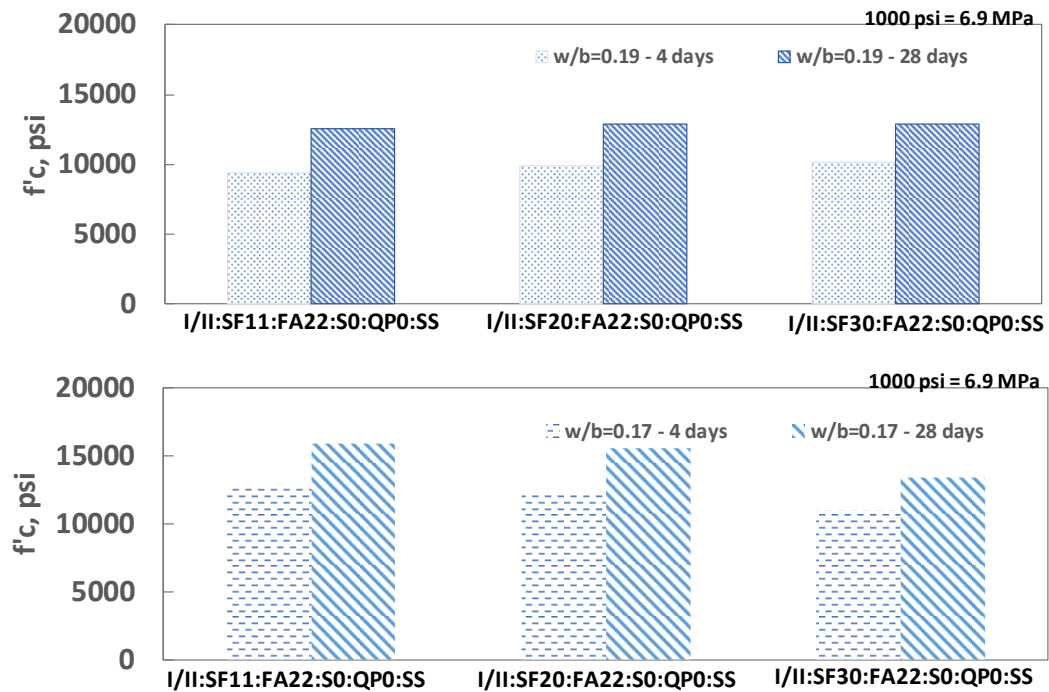
Figure 4.3. Examples of UHPC mixtures with different consistencies

4.2.4 Water-to-binder ratio (w/b)

Water is essential in the fresh state of the concrete to provide sufficient hydration and workability of the cement. Due to the desired high strength and the necessary dense packing of the particles, the w/b of the UHPC was significantly lower than that of conventional concrete. While concrete with a high w/b value generally has high flowability, the portion of water not used for the hydration process will be evaporated later, leaving voids in the matrix, which will have a negative impact on the compressive strength. Thus, the amount of water should be controlled properly to achieve the desired properties. Figure 4.4 shows the flow and compressive strength results of the mixes of stage 2 series 3, prepared with different w/b values.



(a) Flow



(b) Compressive strength

Figure 4.4. Impact of w/b on UHPC performance

While a very low w/b value is necessary for the high strength attributed to UHPC, as mentioned before, a flowable mix is important for UHPC to avoid the entrapment of air, which will have a negative impact on the strength. According to Wille et al. (2011), the increase in the strength can only be associated with the reduction of w/b if the flowability is improved, as implicated by a better packing density. Figure 4.4 shows that, in the mixes that were evaluated, flow decreased when w/b decreased. However, the strength increased in the same series when w/b decreased from 0.19 to 0.17, indicating that a slight decrease in the value of w/b could result in a denser packing, which, in turn, improved the strength. However, although the reduction of w/b improved the strength slightly, the impact on the flow could become a major problem in construction. Thus, the w/b value of approximately 0.19 was chosen. Additional studies should be conducted to define the optimum value of w/b for the UHPC with the materials used. However, due to the limited time, this analysis was not included in this study.

4.3 Results and discussion of the investigation of the binder

4.3.1 Results

The investigation of the binder was conducted in stage 3. The purpose was to study the impact of different types of binders and contents on the fresh and hardened properties of the UHPC. The workability of the concrete was measured based on the spread value of the static flow obtained in the flow table test, and the compressive strength was obtained with the compressive strength test. Table 4.1 presents the flows, unit weights, and compressive strengths of the mixes prepared for the investigation of the binder.

Table 4.1. Results of mixes in the investigation of the binder

| | Mix ID | Flow, in | Unit weight, pcf | $f'_{c,4}$, psi | $f'_{c,14}$, psi | $f'_{c,28}$, psi |
|------------------|-------------------------------------|-------------|------------------------|---------------------|----------------------|----------------------|
| Cement type | I/II: SF11:FA0:S34:QP0:SS | 9.57 | 156.50 | 12958 | 14830 | 17264 |
| | IP: SF11:FA0:S34:QP0:SS | 9.45 | 155.73 | 10021 | 14449 | 15964 |
| | OWH: SF11:FA0:S34:QP0:SS | 6.84 | 158.06 | 8556 | 11554 | 15277 |
| | III: SF11:FA22:S0:QP0:SS | 8.28 | 153.00 | 13436 | - | 16161 |
| Silica fume | I/II: SF11:FA22:S0:QP0:SS | 9.62 | 153.00 | 11416 | 14221 | 14460 |
| | I/II: SF5:FA22:S0:QP0:SS | 8.27 | 153.18 | 11153 | - | 15239 |
| | I/II: SF8:FA22:S0:QP0:SS | 7.52 | 152.73 | 11814 | - | 16729 |
| | I/II: SF11:FA22:S0:QP0:SS | 7.65 | 153.28 | 12349 | - | 17440 |
| | I/II: SF13:FA:22:S0:QP0:SS | 6.25 | 149.38 | 12151 | - | 16611 |
| | I/II: SF16:FA22:S0:QP0:SS | 7.79 | 152.73 | 11703 | - | 16704 |
| | I/II: SF19:FA22:S0:QP0:SS | 7.18 | 150.92 | 11600 | - | 15411 |
| | I/II:UndensifiedSF11:FA22:S0:QP0:SS | 9.93 | 153.5 | 10861 | 12733 | 16127 |
| | I/II:UndensifiedSF11:FA0:S46:QP0:SS | 9.64 | n/a | 11254 | 14614 | 14383 |
| Fly ash | I/II: SF19:FA22:S0:QP0:SS | 7.18 | 150.92 | 11600 | - | 15411 |
| | I/II: SF19:FA16:S0:QP0:SS | 6.87 | 152.10 | 10851 | 13023 | 14841 |
| | I/II: SF19:FA11:S0:QP0:SS | 7.71 | 151.47 | 10986 | 13611 | 15181 |
| | I/II: SF19:FA09:S0:QP0:SS | 7.63 | 151.74 | 11100 | 13031 | 15386 |
| Quartz powder | I/II: SF19:FA0:S0:QP16:SS | 6.19 | 150.59 | 10747 | 13749 | 16057 |
| | I/II: SF19:FA0:S0:QP11:SS | 6.36 | 151.47 | 10656 | 12974 | 14907 |
| | I/II: SF19:FA0:S0:QP9:SS | 6.27 | 153.91 | 11300 | 13174 | 14600 |
| Slag | I/II: SF11:FA0:S23:QP0 | 8.89 | 155.56 | 11777 | 13649 | 16513 |
| | I/II: SF11:FA0:S34:QP0 | 9.57 | 153.91 | 12958 | 14830 | 17264 |
| | I/II: SF11:FA0:S46:QP0 | 9.39 | 156.05 | 15521 | 17093 | 16830 |
| Total Binder | IP: SF11:FA0:S34:QP0:SS:B1500 | 9.45 | 153.91 | 10021 | 14449 | 14456 |
| | IP: SF11:FA0:S34:QP0:SS:B1700 | 10.00 | 155.73 | 11000 | 14489 | 15964 |
| | IP: SF11:FA0:S34:QP0:SS:B1900 | 10.00 | 156.10 | 11396 | 13900 | 16579 |
| | OWH: SF11:FA0:S34:QP0:SS:B1500 | 6.84 | 150.89 | 8556 | 11554 | 15277 |
| | OWH: SF11:FA0:S34:QP0:SS:B1700 | 10.00 | 158.06 | 9517 | 14486 | 16810 |
| | OWH: SF11:FA0:S34:QP0:SS:B1900 | 10.00 | 157.73 | 9956 | 15971 | 17474 |

1 in = 2.54 cm; 1000 psi = 6.9 Mpa; 1 pcf = 16.02 Kg/m³

Note: A flow value of 10.00 indicates that it flowed out of the flow table is less than 2 minutes.

4.3.2 Discussion

a) Impact of the type of cement

Figure 4.5 shows the flow and the compressive strength of series 1 mixes mixed with different types of cement.

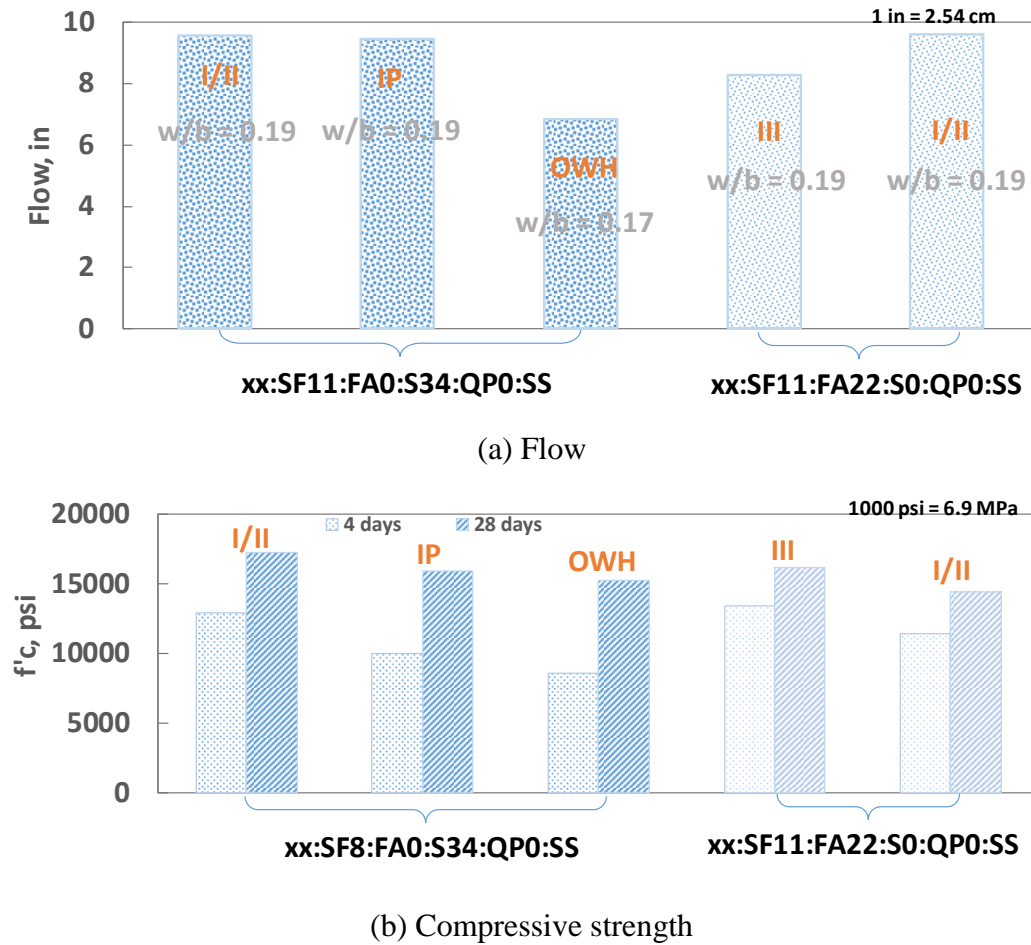


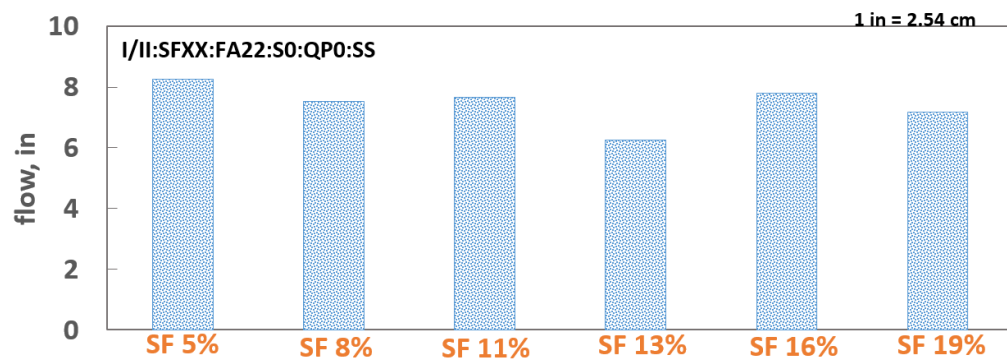
Figure 4.5. Impacts of the types of cement on the performance of the UHPC

Figure 4.5(a) shows that Type I/II and IP cement presented very similar flows, as mentioned before, IP cement consists of 25% Class F fly ash and 75% Type I. However, although fly ash can help the concrete flowability, IP cement has slightly finer particles than Type I/II, which increases the water demand. Due to the coarser particles of class H oil well cement, the surface area decreased, which was believed that less water was required. Thus, a lower w/b was used for this cement than was used for the other types of cement analyzed. However, the Type III cement had finer particles than the other types of cement that were analyzed, and this increased the surface area, which required more water. Since, in this case, the same w/b value was used for both mixes, i.e., with Type III

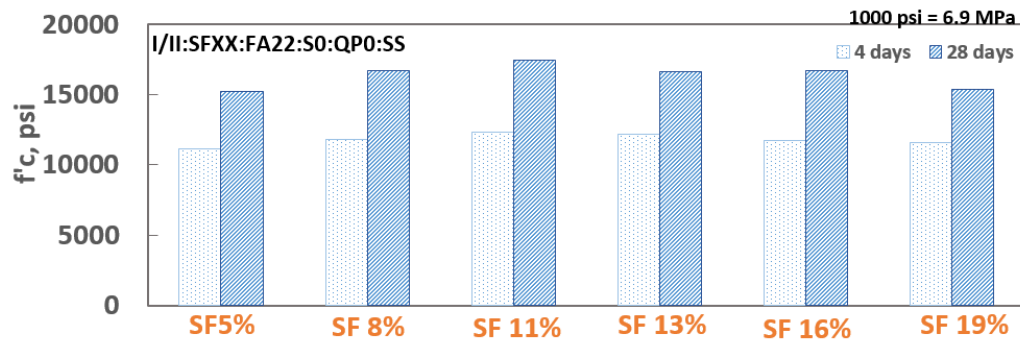
cement and Type I/II cement, the mix with Type III cement had a lower spread value, which led to the conclusion that, when using Type III cement, it would be necessary to increase the w/b in order to increase the concrete flow. The different types of cement that were analyzed presented very similar compressive strength values, which resulted in the selection of Type I/II due to its availability.

b) Impact of silica fume

Series 2 presents the impact of silica fume on the flow and compressive strength of UHPC, and the results are shown in Figure 4.6. The mixes that are presented had the silica fume content, which increased gradually from 5% to 19% with a fixed binder content of approximately 1400 pcy and a fly ash content at 22% of the total binder.



(a) Flow

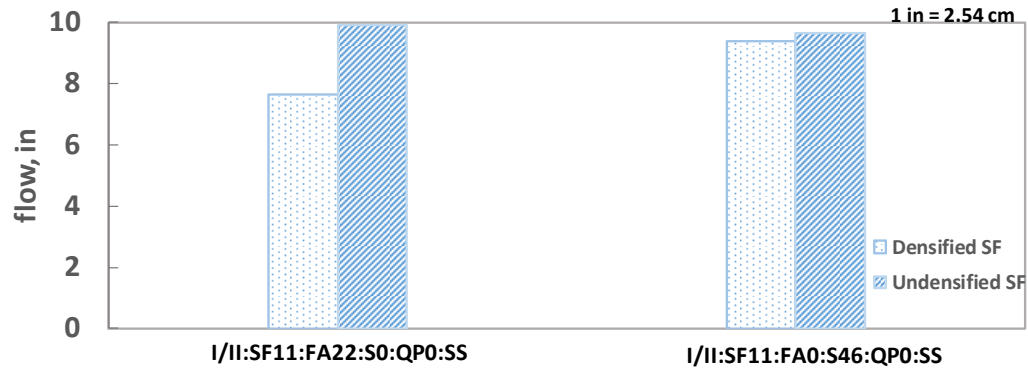


(b) Compressive strength

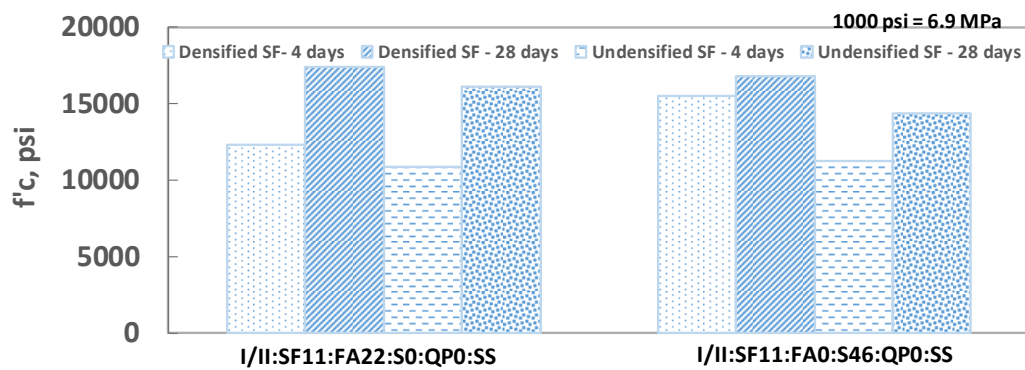
Figure 4.6. Impact of the silica fume content on the performance of the UHPC

Figure 4.6 shows that, when the silica fume content increased, the flow decreased slightly, and the compressive strength increased until it reached a specific value. While it is generally believed that silica fume helps to provide denser particle packing, which, in term, leads to increased strength, it also has a negative impact on the flowability because the particles are very fine. Table 4.1 indicates that the unit weight of concrete with silica fume content ranging between 5% and 11% is higher than that of concrete with the silica fume content ranging between 13% and 19%. The reduction in the unit weight likely is due to the entrapment of air in the slightly lower flowability mixes. Low flowability can result in the entrapment of air in the casting process, which will adversely affect the compressive strength. Thus, the amount of silica fume should be well controlled. Based on the results, the more appropriate dosage of this material for the matrix that was analyzed was 11% of the volume of the total binder. More than 11% will have a negative effect on the flowability and, consequently, the compressive strength, while less than 11% will have a negative effect on the packing of the particles in the matrix, leading to a reduction in the strength.

Figure 4.7 shows a comparison of the impacts of the undensified and the densified silica fume on the flow and compressive strength of the UHPC.



(a) Flow



(b) Compressive strength

Figure 4.7. Comparison of effects of undensified and densified silica fume on the performance of the UHPC

It is apparent that the use of undensified silica fume resulted in a flow that was higher than or similar to that of the densified silica fume. However, when comparing the impacts of the two types of silica fumes on the compressive strength, it is apparent that the strength was reduced when the undensified silica fume was used. This result led to the conclusion that, in this case, the undensified silica fume could have disturbed the packing of the UHPC.

c) Impact of fly ash

Series 3 consists of the effects of fly ash on the flow and compressive strength of the UHPC. The mixes in which the fly ash was analyzed had its content decreased gradually from 22% to 9%. Figure 4.8 shows the results.

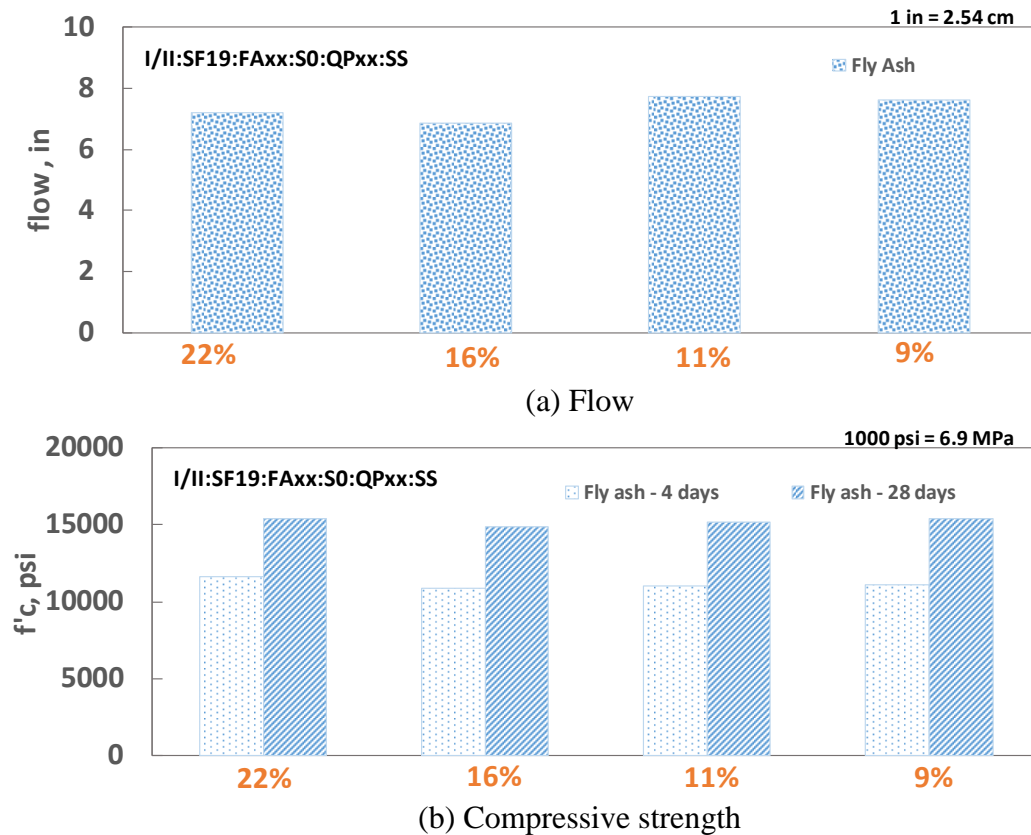


Figure 4.8. Impact of fly ash on the performance of UHPC

Figure 4.8 indicates that the analysis of the fly ash showed that, in general, the decrease in the content of fly ash did not affect significantly the UHPC performance. The flow and the compressive strength slightly decreased as the fly ash content decreased from 22% to 16%. However, the flow slightly increased as the content decreased from 16% to 9% and the strength remained approximately the same.

d) Impact of slag

In Series 4, the impact of slag on the flow and compressive strength of the UHPC was studied, and Figure 4.9 shows the results. The series consisted of mixes with the slag content being increased gradually from 23% to 46%.

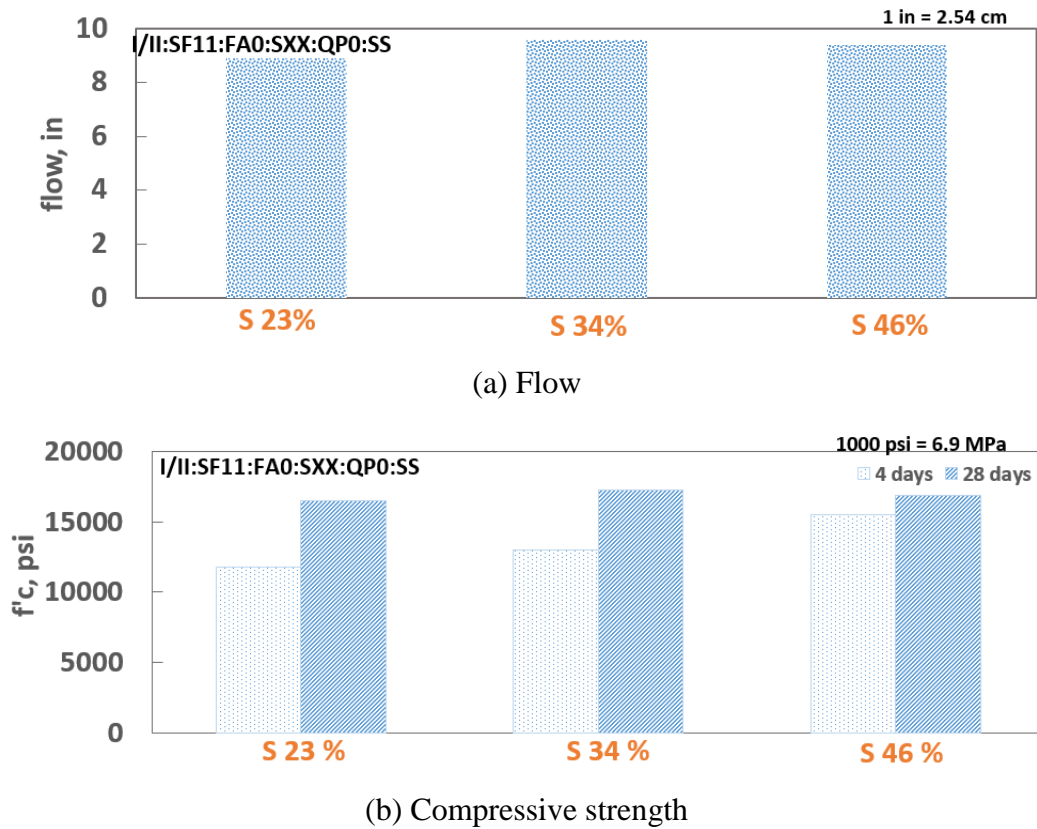


Figure 4.9. Impact of slag on the performance of the UHPC

Figure 4.9 shows that the flow of UHPC increased when the slag content increased from 23% to 34% and that it decreased when the content increased from 34% to 46%. Similar results were observed for the compressive strength of the UHPC. This indicated that the most appropriate content of slag in the mix analyzed was 34% of the total binder by volume. Considering that the mixes had a fixed content of silica fume, as the content of slag increased, the content of cement decreased, and, when slag content

increased by more than 34%, the decrease in the amount of cement began to affect the strength.

e) Quartz powder

Series 5 presents the impact of using quartz powder in the UHPC mix. This series consisted of replacing the fly ash in the mixes from series 3 with quartz powder. Figure 4.10. shows the results.

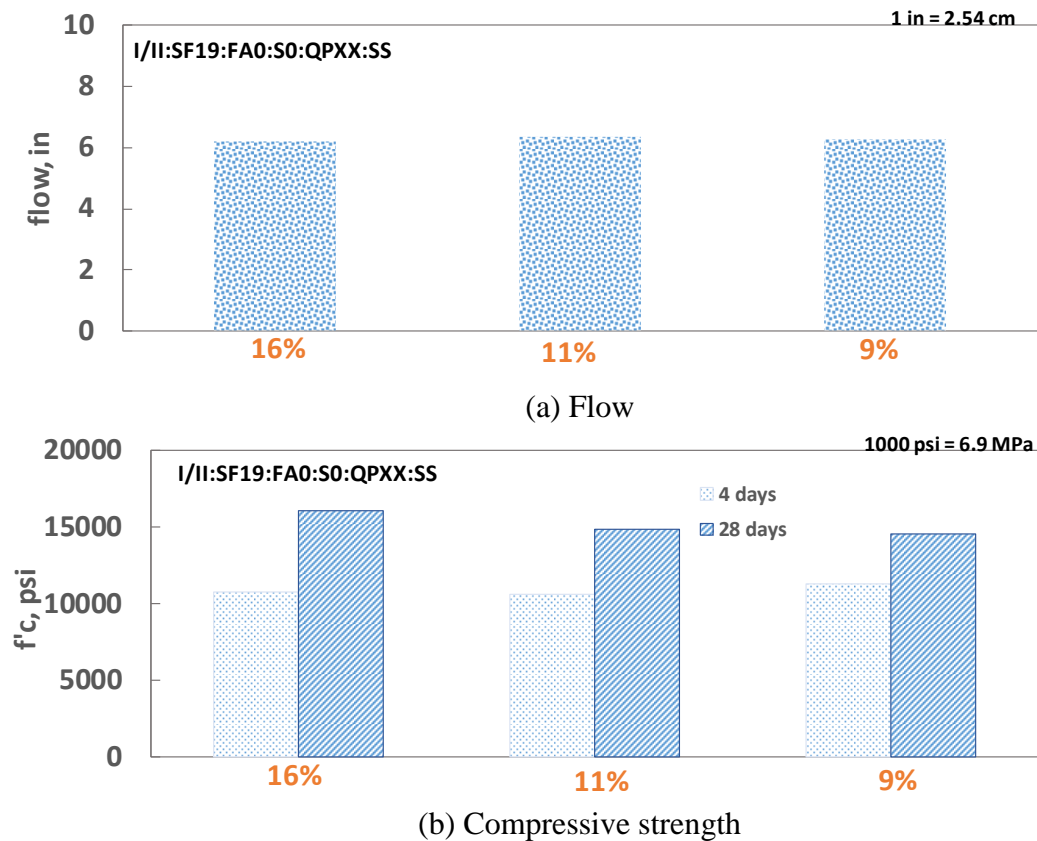


Figure 4.10. Impact of quartz powder in the UHPC performance

Figure 4.10 shows that the reduction of the quartz powder did not affect the overall flowability of the UHPC. However, the 28-day strength slightly decreased when the quartz powder content decreased from 16% to 11% and from 11% to 9%. These

results indicated that the packing density of the UHPC could have decreased as the amount of quartz powder decreased.

When Series 3, the impact of the fly ash in the UHPC, was compared with Series 5, the impact of quartz powder in the UHPC, it was observed that the flow was reduced when quartz powder replaced the fly ash. This reduction was expected because fly ash particles have a spherical shape, and they make it easier for the concrete to flow. Also, quartz powder is a very fine material, so it has a high surface area. Regarding the compressive strength, no significant improvement was observed when the quartz powder replaced the fly ash. However, the combination of the two materials could result in increased strength due to improved packing. The combination of the two materials was not tested in this study.

Comparing I/II:SF8:FA22:S0:QP0:SS (mix with fly ash) with I/II:SF8:FA0:S23:QP0:SS (mix with slag) the flowability is improved when using slag. Even considering that the spherical shape of the fly ash particles facilitates the flowing of the concrete, the increase in the flow when using slag, indicated that its addition could have resulted in an optimized packing. However, the slag and fly ash produced a concrete with very similar results for the 28-day compressive strength.

f) Impact of the content of total binder

The impact of the content of binder was investigated, and the resulting flow and compressive strength of these mixes are shown in Figure 4.11.

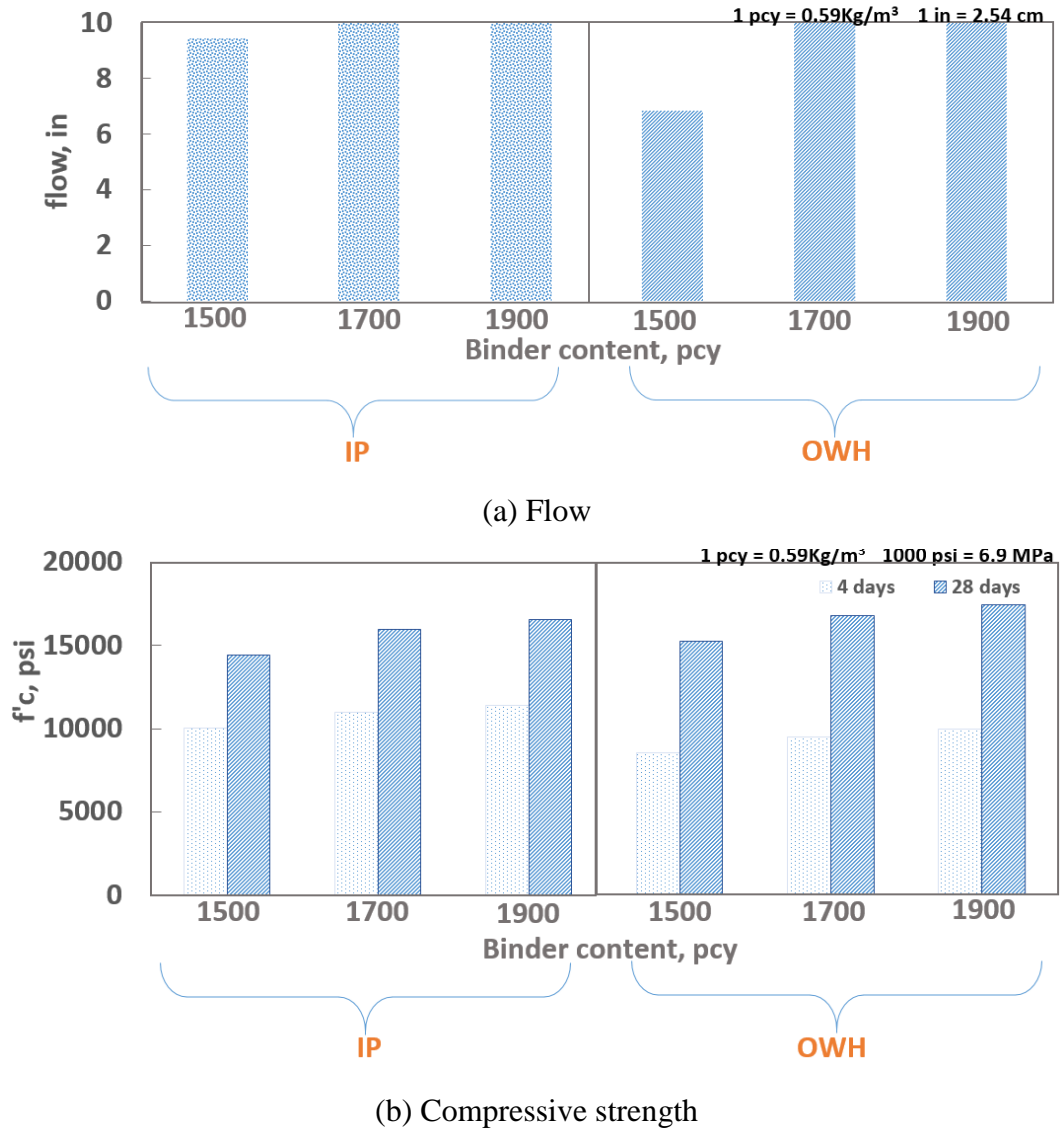


Figure 4.11. Impact of the binder content on UHPC performance

As mentioned previously, as the binder content increases, the paste content of the concrete is increased, leading to a more flowable UHPC. Thus, as expected, the flow of the mixes with the two types of cement increased as the binder content increased (Figure 4.11(a)). Similarly, the compressive strength of the mixes with the two types of cement increased when the binder was increased which resulted in the conclusion that, by the increasing of the paste content, the packing was optimized and more hydration product was formed.

4.4 Particle packing theory

Figure 4.12 shows the theoretical optimum curve and the curves of the mixes prepared with different total binder contents.

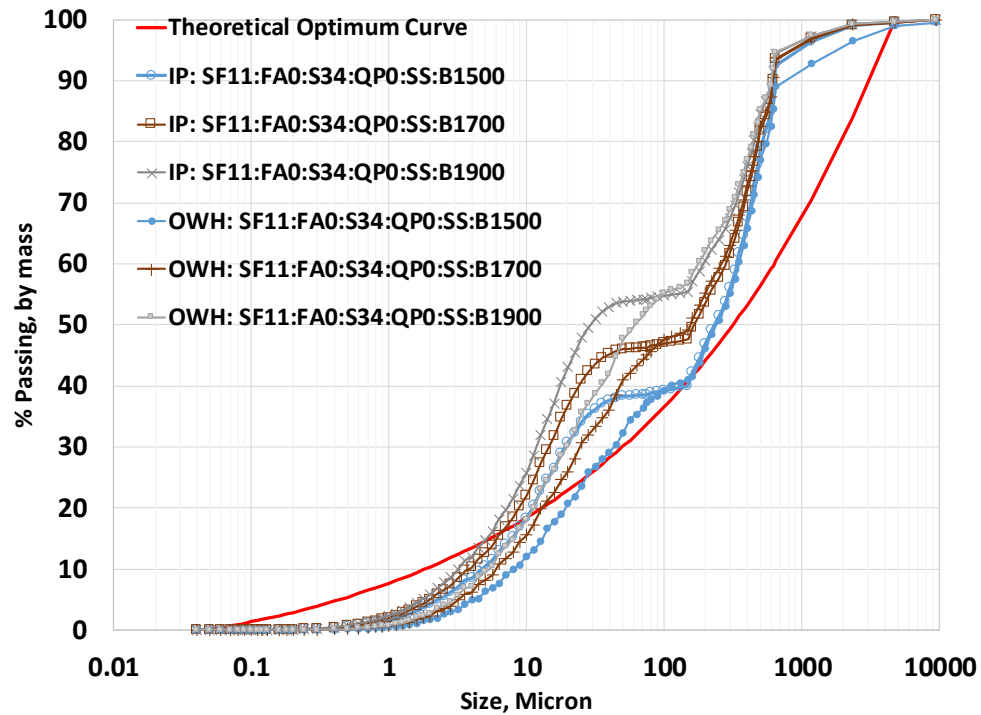


Figure 4.12. Particle packing curve of mixes mixed with different total binder content

Unlike what is presented in the model, the mixes with the best performances were those that had increases in the total content of the binder. The difference that was observed could have been due to the interference of parameters that the model does not account for, such as the interparticle force between fine particles in combination with the use of water and admixtures in the mixes that can affect the forces between fine particles. Moreover, the particle shape and surface condition was not considered in the model. It was concluded that the theoretical packing of the particles does not necessarily result in a UHPC with the highest flow and compressive strength. It is worth noting that besides the

platform portion between 50 and 200 microns, which is the gap of particle sizes between fine aggregate and binders, the particle packing curves also significantly skewed away from the optimum packing curve toward the maximum particle size. While there is only a small (5% to 10%) of particles larger than 0.6mm, presumably all from the No. 10 sand, the particle packing curves can be significantly different. Further study is needed to evaluate the impact of that a small portion of large particles and the gap between aggregate and binder particles.

4.5 Results and discussion of the impact of different mixers and mixing procedures

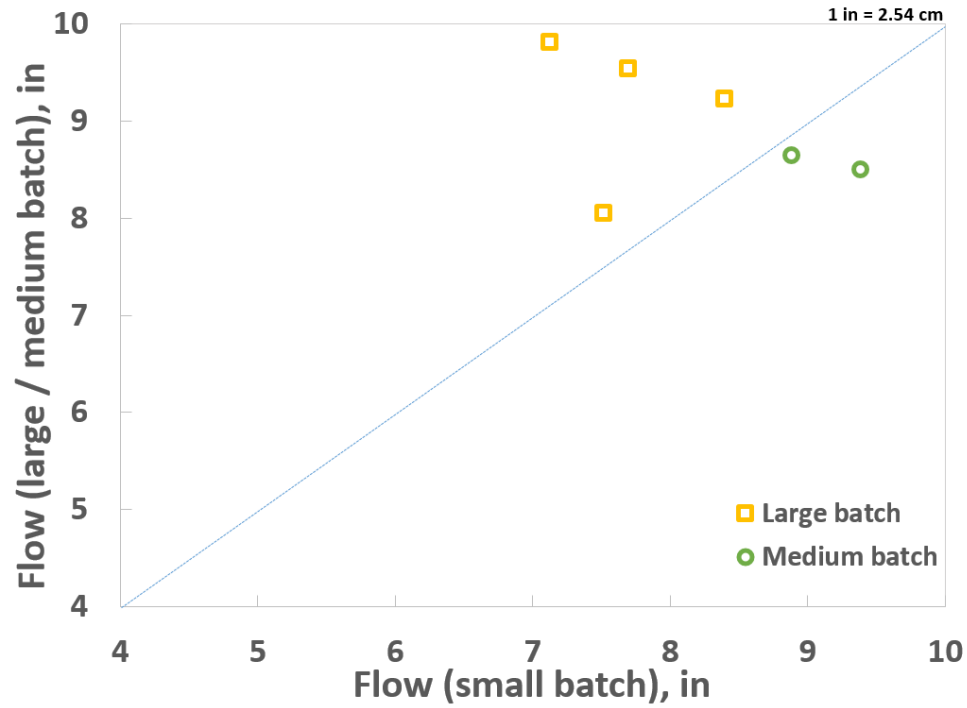
As mentioned earlier, mixing energy is important to properly disperse the materials in UHPC. Thus, stage 4 studied the impacts of different mixers in the UHPC. The four mixes that had different types of fibers were mixed in the small batch volume and the large batch volume. Two mixes from the impact of the slag series (I/II: SF11:FA0:S23:QP0 and I/II: SF11:FA0:S46:QP0) were mixed in the small batch volume and the medium batch volume. The fresh and hardened properties for each of the batches were evaluated, and they are presented in Table 4.2.

Table 4.2. Impact of different mixers

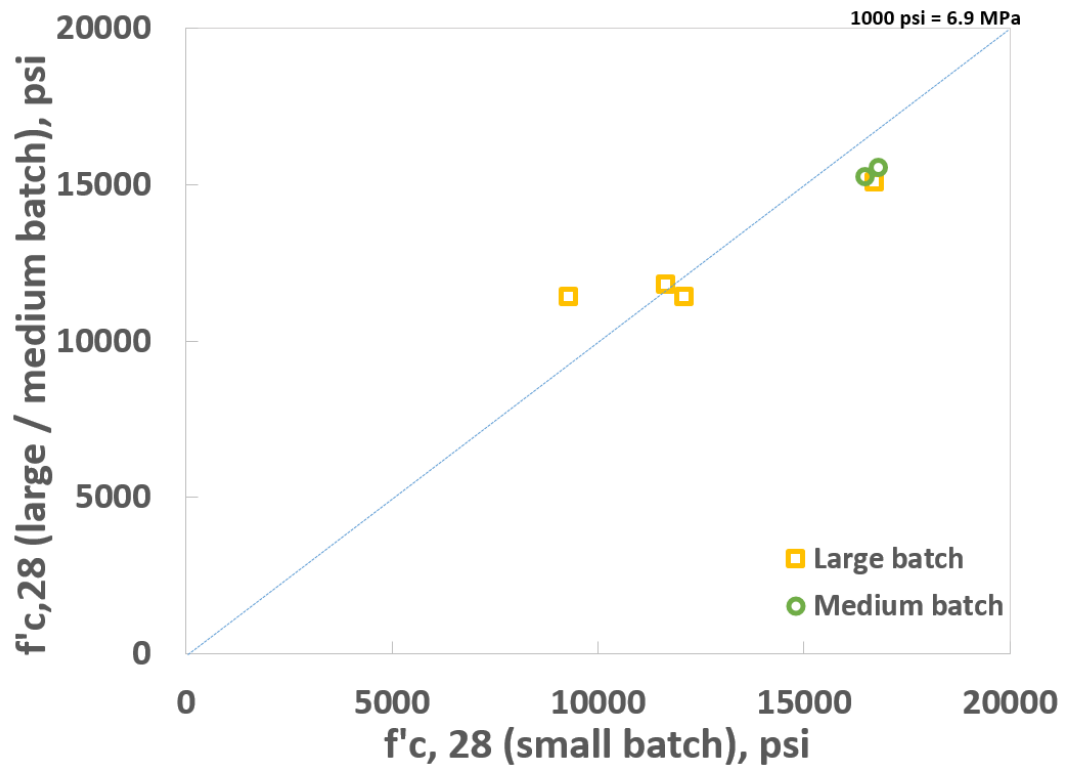
| Mixes ID | Property | Small batch | Medium batch | Large batch |
|----------------------------|-------------------|-------------|--------------|-------------|
| I/II: SF8:FA22:S0:QP0:SS | Flow (in) | 7.52 | - | 8.05 |
| | $f'_{c,28}$ (psi) | 16,729 | - | 15,050 |
| I/II: SF8:FA22:S0:QP0:TS13 | Flow (in) | 7.70 | - | 9.54 |
| | $f'_{c,28}$ (psi) | 9,317 | - | 11,387 |
| I/II: SF8:FA22:S0:QP0:TS25 | Flow (in) | 7.13 | - | 9.81 |
| | $f'_{c,28}$ (psi) | 11,657 | - | 11,777 |
| I/II: SF8:FA22:S0:QP0:SG | Flow (in) | 8.40 | - | 9.23 |
| | $f'_{c,28}$ (psi) | 12,101 | - | 11,387 |
| I/II: SF11:FA0:S23:QP0:SS | Flow (in) | 8.89 | 8.64 | - |
| | $f'_{c,28}$ (psi) | 16,513 | 15214 | - |
| I/II: SF11:FA0:S46:QP0:SS | Flow (in) | 9.39 | 8.50 | - |
| | $f'_{c,28}$ (psi) | 16,830 | 15,530 | - |

1in = 2.54cm; 1000psi = 6.9MPa

Figure 4.13 presented results of the flow and the 28 days compressive strength of small batch mixes compared to both large and medium batches mixes.



(a) Flow



(b) Compressive strength

Figure 4.13. Impact of mixers on the performance of the UHPC

Figure 4.13 shows that, although the mixers have different input energies, UHPC mixed in small, medium, and large mixers resulted in similar values of compressive strength. However, the flow value indicated that the mixtures prepared with the small and large mixers had different flow. The large batch mixes had an average of 1.5 in (38 mm) higher flow than the small batch mixes. The difference likely was due to the higher mixing energy associated with the much larger distances that the large mixing paddles traveled when compared to small paddles. However, the UHPC produced in the medium mixer had an average of 0.57 in (14.5 mm) less flow than the same mixes mixed in the small mixer. This result likely was due to the insufficient dispersion of the materials in the medium mixer in which the paddles were rotating at a much lower speed.

4.6 Summary

Chapter 4 presented the results and discussion of the tests conducted with the UHPC mixes that were prepared. Based on the tests, the materials that resulted in the most promising mixes were selected. The aggregate selected for use was No.10 sand, and the fiber selected was the micro straight steel fiber. The HRWR that provided UHPC with the best performance was the modified polycarboxylate-based HRWR, and the w/b was chosen to be approximately 0.19 to provide the necessary flowability.

For the impact of the cement, types of SCMs, and their contents, results showed that Type I/II cement provided greatest flow and compressive strength in the UHPC mix compared to the other types of cement used. With regard to silica fume content, it was found that 11% by volume of binder was the amount that provides the highest strength. Fly ash and quartz powder did not provide major changes in the UHPC performance and 34% by volume of the binder of slag provided the greater flow and compressive strength.

The total binder content of approximately 1900 pcy provided a UHPC with better performance when compared to the other binder contents analyzed.

CHAPTER 5: SUMMARY, CONCLUSIONS, AND FUTURE WORK

5.1 Conclusions

The objective of this research was to evaluate the impact of different parameters in the development of a UHPC. The UHPC was designed using as much as locally-available materials to the extent possible. The particle packing theory model was used to guide the initial proportions of the materials. However, the impact of each ingredient and impact of the design of the mix on the performance of the UHPC were evaluated experimentally. Based on the results of the study, the following statements can be made:

- Based on results from the initial screening, the aggregate, fiber, HRWR, and w/b that selected for further study was a local fine silica sand (No.10 sand), a straight steel micro-fiber, a modified-polycarboxylate based HRWR, and approximately 0.190, respectively.
- Based on the impact of the type of cement on the performance of the UHPC, it was concluded that the different types of cement had similar impacts on the UHPC. Type I/II cement was selected based on its availability.
- The impact of SCMs on UHPC performance leads to the conclusion that silica fume increases the strength of the UHPC up until approximately 11% (by volume) due to the improvement of particle packing. However, there is no significant improvement after this amount.

- Because of the high variability of the quality of fly ash, slag was deemed a more reliable SCMs and was selected for use in the UHPC mixes. Quartz powder was found not able to improve the strength of UHPC significantly yet negatively affect the workability of UHPC.
- Based on results from the UHPC mixes with Type IP cement and Class H Oil Well cement included in this study, the total binder content used that presented the best results was 1900 pcy.
- With the appropriate mix design and material, it is feasible to develop UHPC with sufficient compressive strength (higher than 17,000psi) and workability (higher than 8 in. flow). However, further study is still needed to identify optimum UHPC design.
- Different mixers do not necessarily influence the mechanical properties of produced UHPC as long as they provide sufficient energy to disperse all of the fine particles of the UHPC design. However, compared with the lab-mixer, the field-scale mixer was found to produce UHPC with slightly higher flowability, which likely was due to the higher mixing energy that was used.
- The modified Andreasen and Andersen particle packing model was used in this study for the initial design. However, the degrees of packing and the findings obtained from the model did not agree with the experimental results. Thus, it was concluded that, while particle packing theory can serve as a general guideline with the specific materials used, experimental work is still necessary to determine the actual packing and to evaluate the impact of materials for the optimum design of UHPC.

5.2 Future work

Since UHPC is still relatively new, additional research is needed to extend the understanding of this complex material. A better understanding of optimum particle packing based on available materials is needed for further mixes development. More rational measurement of workability and rheology is needed to better describe the fresh properties of UHPC. In addition, rheology concept is extremely important to understand and control UHPC behavior including fibers distribution and orientation, stability, and consolidation.

5.2.1 Particle packing and further mixture development

While particle packing theories typically are used to design UHPCs, due to the complexity of the compositions of UHPCs and their interactions and characteristics, the “theoretical optimum particle packing” and the relevant models that calculate the optimum packing might not necessarily provide the best UHPC performance. Firstly, it is believed that an extremely dense packing could block the access of water to the internal powder, and the degree of hydration of the cement could be compromised. Secondly, as there is often a gap between fine aggregate and binder particle sizes, it is not feasible to obtain “optimum” particle packing. A two-stage particle packing model that considers binder and fine aggregate separately might be more appropriate for UHPC design. In addition, the current models do not account for the interactive forces between fine particles, and neither do these models consider the difference between dry particles and wet particles. Water and chemical admixtures can impact the particle size distribution because they may change the interactive forces between the particles. Also, particle packing models do not account for the shapes or the surface textures of particles,

particularly when the fibers are introduced. Besides the modified Andreasen and Andersen, other models should also be considered and evaluated to account for the gaps between fine aggregate and binder particle sizes, and the small portion of particles toward the maximum particle size.

Besides particle packing, a few specific mixtures that could result in improved UHPC performance should be prepared and evaluated. As it was found that the increase of binder content generally results in higher workability, mixtures with high binder content (1900pcy) yet with reduced w/b should be evaluated. Also, as quartz powder is a very fine material that can further improve particle packing; the impact of using slag in combination with quartz powder should be studied.

5.2.2 Rheology of UHPC

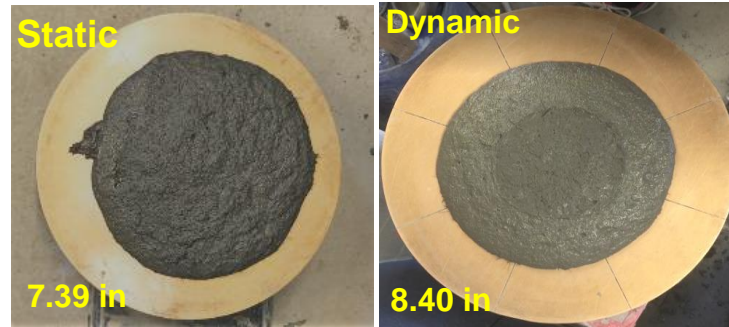
Studies of UHPC rheology can answer questions regarding the distributions of the fibers and their orientation, the flowability of the UHPC in formwork with different geometries, consolidation, time-dependent workability behavior and high thixotropy attributed to UHPC.

5.2.2.1 Workability of UHPC

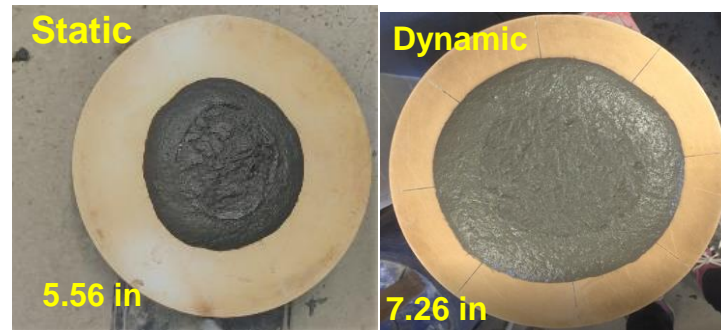
The control of the fresh properties of UHPC requires consistent workability measurements because it directly affects the properties of the hardened material. The properties of fresh UHPC normally are determined using the flow table test. However, as explained in Chapter 2, different procedures for the test have been suggested by different specifications. Two main flow table test methods are being used, i.e., the dynamic flow method and the static flow method. While the dynamic flow method specified dropping the flow table 25 times in 15 seconds and calculating the average of the diameters

measured from the four lines scribed in the table top, the static flow method required that the material be allowed to spread by itself for 2 minutes, followed by calculating the average between the maximum and minimum diameters.

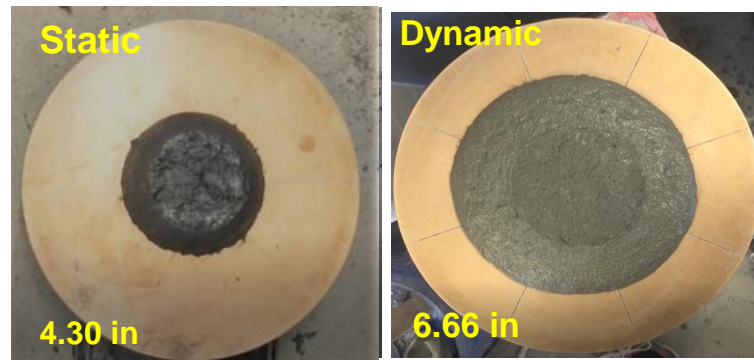
It seems inevitable that these two different methods will provide different results, depending on the UHPC's rheological properties, i.e., viscosity, yield stress, and thixotropy. For instance, Figure 5.1 shows examples of static and dynamic flow results of a selected UHPC mixture with no rest, 3 minutes of rest, and 5 minutes of rest. Figure 5.1 shows that, since UHPC exhibits high thixotropy, the difference of results from the two test methods can provide insights concerning the thixotropy of the material.



(a) No rest



(b) 3-min rest



(c) 5-min rest

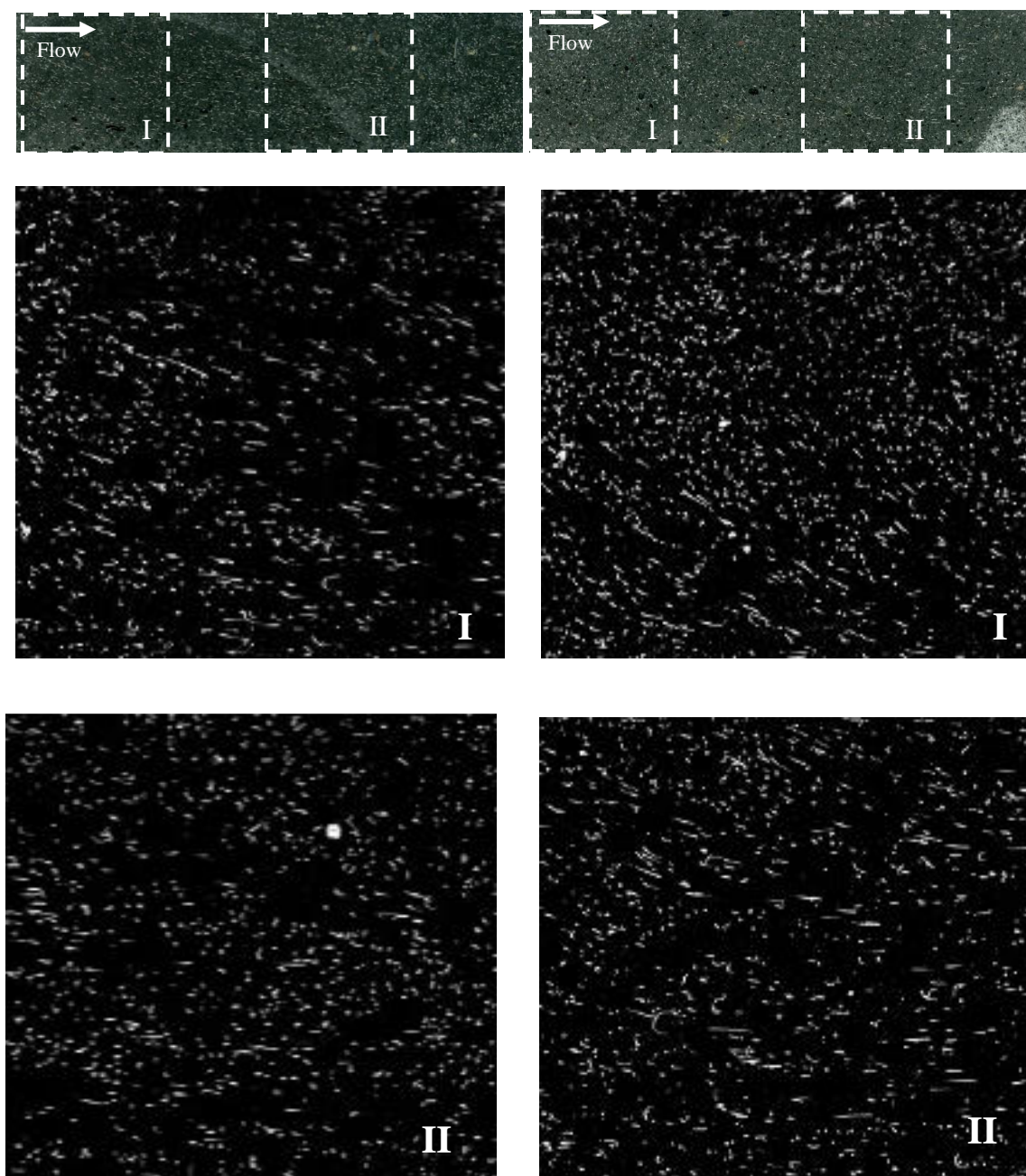
Figure 5.1. Comparison of the results of static and dynamic flow.

With the appropriate use, empirical test methods such as static flow, dynamic flow, and mini V-funnel can be used to reflect the rheological behavior of UHPC in a certain degree. However, to understand better the workability of UHPC, the scientific rheological characteristics obtained from rheometers, such as yield stress and viscosity of

UHPC obtained from rheometer is needed to have a fundamental understanding of the workability of UHPC.

5.2.2.2 Fiber distribution

Research has been conducted to determine the distribution of the fibers in UHPC, and the results have suggested that the self-leveling nature and the viscous consistency align the fibers in the flow direction. Also, it was found that the vibration of UHPC affects the distribution of the fibers (Graybeal, 2014). It is believed that considering the vibration would mostly decrease the yield stress of the concrete and not change its viscosity; the impact of vibration on the orientation of the fibers should not be a concern. However, more study is needed to verify the assumptions and better understand the effects of vibration on UHPC. As an example, Figure 5.2 presents the results from a high-resolution scanner and image process software of a preliminary study on fiber distribution in UHPC prepared with and without vibration. This study showed the differences in the distributions and orientations of the fibers for non-vibrated and vibrated specimens cast with UHPC poured from one end and allowed to flow to the other end.



(a) Not vibrated beam

(b) Vibrated beam

Figure 5.2. Distribution and Orientations of the fibers

Figure 5.2 shows that there was no notable difference in the fibers between the non-vibrated and the vibrated beams. However, it was observed that the fibers do tend to align with the flow.

Another evidence is that within broken beams after the flexural strength test, a similar pattern of the distribution of the fibers was observed in the different specimens that were prepared. Figure 5.3 clearly shows fiber alignment within the cross-section of the beams prepared with same mix design but different types of fibers. Evidentially, the alignment follows the direction in which the UHPC was poured.

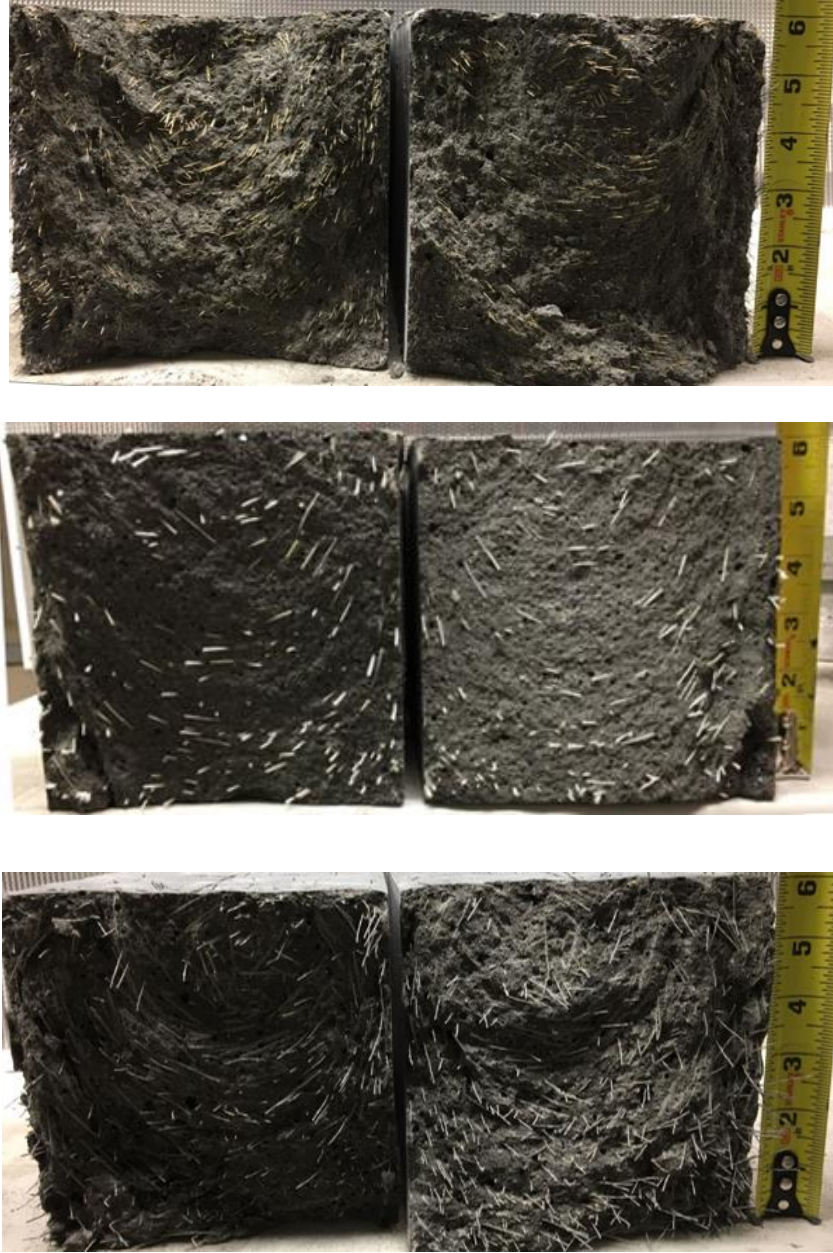


Figure 5.3. Orientations of the fibers in broken beams

The ideal UHPC rheological properties are needed to be defined. The ideal property should provide the required flowability and stability to the concrete and yet allow the fibers to be well distributed.

5.2.2.3 UHPC consolidation

The degree of consolidation of UHPC directly affects the compressive strength of the mix. When the concrete is not well-consolidated, voids can be formed, which has a negative effect on strength. In the course of this study, voids were observed in many specimens. While it is necessary to have a very flowable UHPC in order to ensure appropriate consolidation, it was observed that the high viscosity of the mix can entrap some air voids during casting, leading to poor consolidation. It is necessary to develop a method to cast the UHPC that will minimize the entrapped air.

As an example, a preliminary study of six different types of consolidation processes was conducted. Consolidation process No. 1 consisted of pouring the concrete in the cylinder molds with no tamping or any type of aid to consolidation. Processes No. 2 and No. 3, refer to the process with the cylinders were vibrated externally for 1 minute and 30 seconds respectively, on a vibration table. Process No. 4 consisted of cylinders cast in three layers, and each layer was tapped by hand approximately three times on the walls of the mold. In process No. 5, cylinders were cast in one layer and hand tapped approximately three times in the walls of the molds. Process No. 6 consisted of vibrating the cylinders on the vibration table while casting.

The unit weights of cylinders cast using the six different methods are presented in Table 5.1.

Table 5.1. Concrete unit weight using different consolidation methods

| Process No. | Mix 1 | Mix 2 |
|-------------|-------------------|--------|
| | Unit weight (pcf) | |
| 1 | 149.38 | 147.57 |
| 2 | 155.72 | 151.19 |
| 3 | 153.91 | 151.19 |
| 4 | 154.81 | 153.00 |
| 5 | 150.29 | 152.10 |
| 6 | 154.81 | 153.00 |

1 pcf = 16.02 Kg/m³

As shown in Table 5.1, processes No. 4 and No. 6 appear to provide the most effective consolidation. However, a systemically study with different casting methods for UHPC mixes with different rheological properties is needed to determine which process will be more effective in minimizing the formation of entrapped air.

CHAPTER 6: REFERENCES

1. Alkaysi, M., and El-Tawil, S. Effects of Variations in the Mix Constituents of Ultra High Performance Concrete (UHPC) on Cost and Performance. *Material and Structures* (66), 2015.
2. Ambily, P. S., Ravisankar, K., Umarani, C., Dattatreya, J. K., and Iyer, N. R. Development of Ultra-High-Performance Geopolymer Concrete. *Magazine of Concrete Research - Institute of Civil Engineers* (66(2)), 2014. 82:89.
3. American Concrete Institute ACI. Ultra-High-Performance Concrete: *An Emerging Technology Report* (Committee 239), 2018
4. American Petroleum Institute API (Spec 10A). *Specification for Cement and Materials for Well Cementing*, 2010.
5. ASTM C1240. Standard Specification for Silica Fume Used in Cementitious Mixtures. *ASTM International*, 2015.
6. ASTM C1252. Standard Test Methods for Uncompacted Void Content of Fine Aggregate *ASTM International*, 2012
7. ASTM C136. Standard Test Method for Sieve Analysis of Fine and Coarse Aggregates. *ASTM International*, 2014.
8. ASTM C1437. Standard Test Method for Flow of Hydraulic Cement Mortar. *ASTM International*, 2015.
9. ASTM C150. Standard Specification for Portland Cement. *ASTM International*, 2018.
10. ASTM C1609. Standard Test Method for Flexural Performance of Fiber-Reinforced Concrete (Using Beam with Third-Point Loading). *ASTM International*, 2012.

11. ASTM C1017. Standard Specification for Chemical Admixture for Use in Producing Flowing Concrete. *ASTM International*, 2013.
12. ASTM C1856. Standard Practice for Fabricating and Testing Specimens of Ultra-High Performance Concrete. *ASTM International*, 2017.
13. ASTM C1856. Standard Practice for Fabricating and Testing Specimens of Ultra-High Performance Concrete. *ASTM International*, 2017.
14. ASTM C230. Standard Specification for Flow Table for Use in Test of hydraulic Cement. *ASTM International*, 2014.
15. ASTM C494. Standard Specification for Chemical Admixture for Concrete. *ASTM International*, 2017.
16. ASTM C595. Standard Specification for Blended Hydraulic Cements. *ASTM International*, 2018.
17. ASTM C618. Standard Specification for Coal Fly Ash and Raw or Calcined Natural Pozzolan for Use in Concrete. *ASTM International*, 2017.
18. ASTM C989. Standard Specification for Slag Cement for use in Concrete and Mortar. *ASTM International*, 2018.
19. Berry, M., Snidarich, R., Wood, C. Development of Non-Proprietary Ultra-High Performance Concrete. *The State of Montana Department of Transportation FHWA/MT-17010/8237-001*, 2017.
20. Bonneau, O., Lachemi, M., Dallaire, E., Dugat, J., and Aitcin, P. Mechanical Properties and Durability of Two Industrial Reactive Powder Concretes. *ACI Materials Journal*, 1997. 286:290

21. Choi, M. S., Lee, J. S., Ryu, K. S., Koh, K., and Kwon S. H. Estimation of Rheological Properties of UHPC Using Mini Slump Test. *Construction and Building Materials* (106), 2016. 632:639.
22. De Larrard, F. and Sedran, T. Optimization of Ultra-High-Performance Concrete by the Use of Particle Packing. *Cement and Concrete Research*, 1994. 997:1009.
23. De Larrard, F. Concrete Mixture Proportioning a Scientific Approach. *Taylor & Francis*, 1999.
24. Diamond, S. and Sahu, S. Densified Silica Fume: Particle Sizes and Dispersion in Concrete. *Materials and Structures* (39), 2006. 849:859.
25. Dils, J., Boel V., and De Schutter. G. Influence of Cement Type and Mixing Pressure on Air Content, Rheology and Mechanical Properties of UHPC. *Construction and Building Materials* (41), 2013. 455:463.
26. El-Tawil, S., Alkaysi, M., Naaman A., Hansen W., and Liu Z. Development, Characterization and Applications of a Non Proprietary Ultra High Performance Concrete for Highway Bridges. *Department of Civil and Environmental Engineering University of Michigan, Ann Arbor, Michigan*. 2016.
27. El-Tawil, S., Tai, Y., Meng, B., Hansen W., and Liu, Z. Commercial Production of Non-Proprietary Ultra-High Performance Concrete. *Michigan Department of Transportation* (RC-1670), 2018.
28. Fedorsian, I., and Camoes, A. Effective Low-Energy Mixing Procedure to Develop High-Fluidity Cementitious Pastes. *Materia Rio de Janeiro*, 2016.
29. Graybeal, B., and Hartmann, J. Strength and Durability of Ultra High Performance Concrete. *Presented at Concrete Bridge Conference*, 2003.

30. Graybeal, B. Design and Construction of Field-Cast UHPC Connection. *Federal Highway Administration Tech Note FHWA-HRT-14-084*, 2014.
31. Graybeal, B. Development of Non-Proprietary Ultra High Performance Concrete for Use in the Highway Bridge Sector. *Federal Highway Administration*, FHWA –HRT-13-100, 2013.
32. Haber Z. B., De la Varga, I., Graybeal, B., Nakashoji, B., and El-Helou, R. Properties and Behavior of UHPC-Class Materials. *Federal Highway Administration*, FHWA-HRT-18-036, 2018.
33. Holland T. C. Silica Fume User's Manual. *Federal Highway Administration FHWA-IF-05-016*, 2005.
34. Hunger, M. An Integral Design Concept for Ecological Self-Compacting Concrete. *Eindhoven University of Technology, Netherlands*, 2010.
35. Hunger, M., and Brouwers, J. Development of Self-Compacting Eco-Concrete. *Presented at 16th International Conference on Building Materials, Weimar, Germany*, 2006.
36. Japan Society of Civil Engineers. Recommendation for Design and construction of High Performance Fiber Reinforced Cement Composites with Multiple Fine Cracks (HPFRCC), 2008.
37. Khayat, K. H., and Meng, W. Design and Performance of Stay-in-Place UHPC Prefabricated Panels for Infrastructure Construction. *Center for Transportation Infrastructure and Safety*, 2014.
38. Kosmatka, S. H., Kerkhoff, B., and Panarese, W. C. Design and Control of Concrete Mixtures (14th.). United States of America: Portland Cement Association.

39. Lowke, D., Stengel, T., Schiebl, P., and Gehlen, C. Control of Rheology, Strength and Fibre Bond of UHPC with Additions- Effect of Particle Density and Addition Type. *3rd International Symposium on “UHPC and Nanotechnology or High Performance Construction Materials”*, Kassel, 2012.
40. Meng, W. Design and Performance of Cost-Effective Ultra-High Performance Concrete for Prefabricated Elements. *Missouri University of Science and Technology, Doctoral Dissertation*, 2017.
41. Meng, W., and Khayat, K. H. Mechanical Properties of Ultra-High-Performance Concrete Enhanced With Graphite Nanoplatelets and Carbon Nano Fibers. *In Composites Part B* (107), 2016. 113:122.
42. Meng, W., and Khayat, K. H. Improving Flexural Performance of Ultra-High Performance Concrete by Rheology Control of Suspending Mortar. *Composites Part B* (117), 2017 (a). 26:34.
43. Meng, W., Valipour, M., and Khayat, K. H. Optimization and Performance of Cost-Effective Ultra-High Performance Concrete. *Materials and Structure*, 2017 (b). 50:29.
44. Muzenski, W. S. The Design of High performance and Ultra-High Performance Fiber Reinforced Cementitious Composites with Nano Materials. *University of Wisconsin-Milwaukee. A Doctoral Dissertation*, 2015.
45. Naaman, A., and Wille, K. The Path to Ultra High Performance Fiber Reinforced Concrete (UHP-FRC): Five Decades of Progress. *In proceedings of Hipermat 2012, 3rd International Symposium, “Ultra High Performance Concrete and Nanotechnology in Construction”*, Germany, 2012.

46. National Precast Concrete Association. Ultra High Performance Concrete (UHPC) – Guide to Manufacturing Architectural Precast UHPC Elements NCPA, n/a.
47. Sakai, E., Akinori, N., Daimon, M., Aizawa, K., and Kato, H. Influence of Superplasticizer on the Fluidity of Cements with Different Amount of Aluminate Phase. *Second International Symposium on Ultra High Performance Concrete, Kassel, Germany*, 2008. 85:92.
48. Sbia, L. A., Peyvandi, A., Soroushian, P., and Balachandra, A. M. Optimization of Ultra-High-Performance Concrete with Nano- and Micro-Scale Reinforcement. *Cogent Engineering*, 2014. 1:11.
49. Schroefl, C., Gruber, M., and Plank, J. Structure Performance Relationship of Polycarboxylate Superplasticizers Based on Methacrylic Acid Ester in Ultra High Performance Concrete. *Second International Symposium on Ultra High Performance Concrete, Kassel, Germany*, 2008. 383:390.
50. Scott, A. D., Long, W. R., Moser R. D., Green, B. H., O'Daniel, J. L., and Williams, B. A. Impact of Steel Fibers Size and Shape on the Mechanical Properties of Ultra-High Performance Concrete. *U. S. Army Corps of Engineers Washington*, (DC 20314-1000 ERDC/GSL TR-15-22), 2015.
51. Scrivener, K. L., Crumbie, A. K., and Laugesen, P., The Interfacial Transition Zone (ITZ) Between Cement Paste and Aggregate in Concrete. *Interface Science* (12(4)), 2004. 411:421.
52. Shi, C., Wu, Z., Xiao, J., Wang, D., Huang, Z., and Fang, Z. A Review on Ultra High Performance Concrete: Part I. Raw Materials and Mixture Design. *Construction and Building Materials* (101), 2015. 741:751

53. Wille, K., Naaman, A. E., and Parra-Montesinos, G. J. Ultra High Performance Concrete with Compressive Strength Exceeding 150MPa (22KSi): A Simpler Way. *ACI Material Journal*, 2011 (a). 46:54.
54. Wille, K., Naaman, A. E., and El-Tawil, S. Optimizing Ultra-High-Performance Fiber-Reinforced Concrete, Mixtures with Twisted Fibers Exhibit Record Performance under Tensile Loading. *Concrete International*, 2011 (b). 35:41.
55. Wu, Z., Shi, C., Khayat, K. H., and Wan, S. Effect of Different Nanomaterials on Hardening and Performance of Ultra-High Strength Concrete (UHSC), *Cement and Concrete Composites* (70), 2016. 24:34.
56. Yang, S. L., Millard, S. G., Soutsos, M. N., Barnett, S. J., and Le, T. T. Influence of Aggregate and Curing Regime on Mechanical Properties of Ultra High Performance Concrete. *Construction and Building Materials* (23), 2009. 2291:2298.
57. Yu, R., Spiesz, P., and Browsers, H. J. H. Effect of Nano-Silica on the Hydration and Microstructure development of Ultra-High Performance Concrete (UHPC) with a Low Binder Amount. *Construction and Building Materials* (65), 2014 (a). 140:150.
58. Yu, R., Spiesz, P., and Browsers, H. J. H. Mix design and Properties Assessment of Ultra-High Performance Fibre Reinforced Concrete (UHPFRC). *Cement and Concrete Research* (56), 2014 (b). 29:39.
59. Yu, R., Spiesz, P., and Browsers, H. J. H. Development of an Eco-Friendly Ultra-High Performance Concrete (UHPC) With Efficient Cement and Mineral Admixture Uses. *Cement and Concrete Composites* (55), 2015. 383:394.